MULTIMODAL BIOMETRIC ANALYSIS
FOR MONITORING OF WELLNESS

by

Vahan V. Grigoryan

Diploma in Mathematics, Yerevan State University, 1997

M.A. in Mathematics, University of Pittsburgh, 1999

M.S. in Information Science, University of Pittsburgh, 2004

Submitted to the Graduate Faculty of

the School of Arts and Sciences in partial fulfillment

of the requirements for the degree of

Doctor of Philosophy

University of Pittsburgh

2004

UNIVERSITY OF PITTSBURGH

SCHOOL OF ARTS AND SCIENCES

This dissertation was presented

by

Vahan V. Grigoryan

It was defended on

December 6, 2004

and approved by

Gregory M. Constantine, Professor, Department of Mathematics

Donald M. Chiarulli, Professor, Department of Computer Science

G. Bard Ermentrout, University Professor, Department of Mathematics

Robert W. Heath, Professor, Department of Mathematics

Milos Hauskrecht, Assistant Professor, Department of Computer Science

Dissertation Advisors: Gregory M. Constantine, Professor, Department of Mathematics,

Donald M. Chiarulli, Professor, Department of Computer Science

ABSTRACT

MULTIMODAL BIOMETRIC ANALYSIS
FOR MONITORING OF WELLNESS

Vahan V. Grigoryan, PhD

University of Pittsburgh, 2004

Biometric data can provide useful information about a person's overall wellness. The focus of this dissertation is wellness monitoring and diagnostics based on behavioral and physiological traits. The research is comprised of three studies: passive non-intrusive biometric monitoring, active monitoring using a wearable computer, and a diagnostics of early stages of Parkinson's disease.

In the first study, a biometric analysis system for collecting voice and gait data from a target individual has been constructed. The central issue in that problem is the filtering of the data that is collected from non-target subjects. A novel approach to gait analysis using floor vibrations has been introduced. Naive Bayes model has been used for gait analysis, and the Gaussian Mixture Model has been implemented for voice analysis. It has been shown that the designed biometric system can provide sufficiently accurate data stream for health monitoring purposes.

In the second study, a universal wellness monitoring algorithm based on a binary classification model has been developed. It has been tested on the data collected with a wearable body monitor SenseWear®PRO and with Support Vector Machines acting as an underlying binary classification model. The obtained results demonstrate that the wellness score produced by the algorithm can successfully discriminate anomalous data.

The focus of the final part of this thesis is an ongoing project, which aims to develop an automated tool for diagnostics of early stages of Parkinson's disease. A spectral measure of balance impairment has been introduced, and it has been shown that that measure can separate the patients with Parkinson's disease from control subjects.

TABLE OF CONTENTS

LIST OF TABLES

LIST OF FIGURES

PREFACE

This thesis would have been impossible without help and support of many people. First and foremost of all, I would like to thank my advisors Donald Chiarulli and Gregory Constantine for their guidance and patience throughout all these years. I am grateful to Dr. Chiarulli that he gave me resources and independence for conducting my research. I am indebted to Dr. Constantine for his invaluable support and encouragement.

Thanks to Milos Hauskrecht for pointing me in the right direction at the time when I was lost. The numerous meetings and discussions with him have been a great source of inspiring ideas. I would also like to thank the other members of the committee, Bard Ermentrout and Robert Heath, for their constructive and helpful comments.

Thanks to Sava Denev for convincing me to type this thesis in LaTeX and sending me helpful tips and advices about it. I am obliged to Seda Avetisian and Sharon McDerrmott for reading the manuscript and correcting my English. Thanks to Dave Andre and Bodymedia, Inc. for allowing me to use their data in the wellness monitoring simulations.

Thanks to all of my friends in Pittsburgh, who made the graduate student life more tolerable. Special thanks to Leo Selavo, Jose Martinez, and Majd Sakr, for their interesting questions about my research and their valuable comments about my presentation skills.

At last, I would like to thank my parents for their continued love and support and for encouraging me to pursue my goals halfway across the globe. I can never thank them enough for teaching me to value education and for feeding my curiosity since I was little.

1.0 INTRODUCTION AND MOTIVATION

As people age, our learning abilities, senses, as well as other organs begin to fail. Elderly people often require assistance even in their simplest daily activities, and the number of those who are in need of care is increasing. As the baby-boomer generation approaches the retirement age, by 2030, more nearly 20% of the population will be 65 and over [1]. Health care costs are increasing at a high rate, and there is a serious shortage of nurses. These factors indicate that the problem cannot be tackled with a conventional approach, and there is a need for new means of elderly care.

In the 21st century, computers and robots are present in many aspects of our lives. They are used in factories, offices, schools, and museums. Thus, it would be logical to try using robots and wearable computers to provide personalized care and automated diagnostics for the elderly and disabled.

This dissertation describes three applications of machine learning and data mining techniques to wellness monitoring and diagnostic problems. The first problem is the design of passive non-intrusive biometric monitoring system for collecting voice and gait data in the context of the Nursebot project. The second problem is active wellness monitoring using physiological and behavioral data collected with a wearable body monitor. The third application deals with the problem of early diagnostics of Parkinson's disease using a force platform data.

1.1 BIOMETRIC ANALYSIS

People have always used biological traits, such as voice, face, gait, etc. to recognize each other. The technological revolution of the 20th century and recent developments of mathematical apparatus in machine learning and pattern classification created opportunities for automatic person recognition using biological traits. Biometrics emerged as an automated method of identifying individuals or verifying the identity of a person based on distinctive physiological or behavioral characteristics.

When we observe biometric traits of familiar people, such as friends or relatives, we can often make conclusions beyond recognition. We can guess that a person has had little sleep by his face, or that he has a cold by his voice, or that his leg hurts because he is limping. Thus, it is quite natural to build a biometric analysis system that will try to assess a person's wellness by his/her behavioral and/or physiological traits.

From some of the physiological traits like fingerprints or the iris, one cannot obtain much information about a person's wellness. Other physiological traits, such as pulse or heartbeat, have been used in medicine for thousands of years as an effective indicator of a patient's condition. Continuous acquisition of physiological data usually requires wearable sensors, while behavioral traits, such as voice and gait, can be monitored without disturbing the person.

1.2 NURSEBOT PROJECT

The "Nursebot Project" is a collaborative effort of the researchers at the University of Pittsburgh, Carnegie Mellon University, and the University of Michigan, which aims to develop a mobile robotic assistant for elderly people in order to allow them to maintain independent living and avoid institutionalization. One of the functions of the Nursebot is the systematic monitoring of wellness with biometric sensors. Since some people are sensitive about intrusion into their life, and since the Nursebot will be collecting biometric data continuously, it is important to do that inconspicuously.

It is well known that the health problems can be effectively treated if they are detected early. The health of the elderly is particularly fragile; thus, it is especially important to identify even smallest changes in their condition. The chances of detecting those will significantly increase if doctors had more data about patients health, than that collected during an appointment or a visit. Therefore, the data available through passive monitoring of wellness with the Nursebot will give a better idea of a patient's condition to doctors and nurses.

The non-intrusion constraint in the Nursebot project limits the choice of biometric traits that will be monitored by the robot mainly to behavioral traits, such as voice and gait, versus physiological traits, such as temperature or heartbeat. It also opens a very important question regarding the source of the collected data. The data collected from the person who is being monitored needs to be separated from the data that is collected from other people who are in the same environment. We will refer to the latter data as *biometric noise.*

The goal of the first problem discussed in this thesis is to build a **biometric analysis system** that collects behavioral data using multiple sensors with no direct communication with the subject and filters out the biometric noise in order to produce a reliable signal for further examination. The main components of the system are:

1. **Data acquisition.** The system is based on gait and voice data. Two microphones and one microaccelerometer are used for data acquisition. The accelerometer and one of the microphones collect the data about person's gait, and the other microphone is used to collect the speech data.
2. **Feature extraction.** The purpose of feature extraction is to produce low dimensional feature vectors that emphasize those properties of the data which are important for the classification task at hand.
3. **Filtering of the non-subject data.** This component classifies the data into "genuine" (collected from the target subject) and "impostor" (biometric noise) classes.

The design of our biometric analysis system is based on machine learning and pattern recognition techniques. A pattern recognition system based on a supervised learning model requires a *training* phase [2]. During that phase, the system is provided with both sample features and an expected output for each feature. This way the system "learns" the prop-

erties of the target subject. Later, during the recognition phase, the system uses that prior knowledge about the target subject in order to classify and analyze the unknown data.

The problem of filtering of the non-subject data is related to the problem of machine recognition of human subjects based on biometric data. Biometric recognition can be used in two modes: identification and verification [3]. *Identification* mode is used when we need to identify the person by matching his/her biological traits with the entire population in the database; it essentially answers the question, "Whose biometric data is this?". *Verification* mode is used when the system authenticates the person's claimed identity by comparing his/her biometric characteristics with the ones stored in the database; in other words, the system answers the question, "Does this biometric data belong to the person it claims to belong?"

However, our problem has several important differences. The first difference from a typical biometric recognition problem is that we can tolerate a large number of true negative errors. That is because we deal with long term monitoring of the subject, thus, we have access to a large amount of genuine data and low sample rate is not an issue for our system. Another difference is that the Nursebot is going to operate in an eldercare environment. The number of people in that universe will likely be limited to family members, friends, and caregivers. This puts an upper bound to a number of people our system may expect to detect besides the target subject. Finally, the system uses multiple sensors; therefore, the final decision can be made by integration of information received from each of them.

1.3 WEARABLE BIOMETRIC MONITOR

The integration of physiological and behavioral information from multiple sensors is the central idea in SenseWear®PRO, a wearable body monitor developed by a Pittsburgh-based company BodyMedia [4]. SenseWear®PRO monitor uses its six sensors to continuously gather data on movement, heat flow, skin temperature, ambient temperature, and galvanic skin response of the subject. It is worn on the back of the upper arm, and it is equipped with wireless interface which enables data transfer without removing the device from the subject.

The goal of the second problem discussed in this thesis is to develop a **wellness monitoring algorithm** and test it on the data collected with SenseWear®PRO. The experimental design for testing of the algorithm is as follows:

1. **Data acquisition.** More than 1500 hours of annotated data from SenseWear®PRO monitor has been available from BodyMedia. It has been provided in the form of nine channels, each sample of which represents one minute of aggregate sensor data.

2. **Feature extraction.** The stepwise backward elimination method is applied in order to exclude the channels that deteriorate the classification accuracy.

3. **Extraction of context activity.** A binary classifier is used for recognition of the data corresponding to the target activity.

4. **Wellness monitoring.** The subject model has been constructed based on a binary classifier and the target activity data. The wellness score is produced by comparing the current subject model with the previous models.

The monitoring algorithm implemented in this thesis does not depend on either features or the classification method; therefore, it can be applied in any data monitoring system, in which the underlying binary recognition model is successful at classifying the target data from a given set of mixed data. Particularly, it can be used for wellness monitoring in the biometric analysis system of the Nursebot.

1.4   MEASURE OF BALANCE IMPAIRMENT

Parkinson's disease (PD) is a progressive neurological disorder caused by the death of dopamine-producing cells in the brain. The major symptoms of PD are motion impairment, resting tremor, rigidity, bradykinesia (slowness of movement), akinesia (difficulty in movement initiation), and postural instability [5, 6]. About one million Americans are affected by PD, making it second most common neurodegenerative disorder after Alzheimer's disease [7].

Presently, Parkinson's disease and its severity are diagnosed symptomatically by physicians using standard clinical rating scales, such as the Unified Parkinson's Disease Rating Scale (UPDRS) [8]. The diagnosis and progression level can also be assessed using expensive and somewhat unpleasant brain imaging techniques, such as computerized tomography (CT), positron-emission tomography (PET), and single photon emission computed tomography (SPECT) [9, 10]. In early stages of PD, when clinical symptoms are mild, those techniques are currently the only way of detecting the disease. Early diagnosis of PD is highly desirable, since early treatment may slow the progression of the disease [11].

The goal in the last problem presented in this thesis is to **develop a measure of balance impairment** using data collected with an electronic force platform, which can be used for early diagnostics of Parkinson's disease. This is still an ongoing project, but the preliminary results presented in the Chapter 5 demonstrate that the spectral features obtained from the force platform data can discriminate the patients with PD from control subjects.

1.5   DISSERTATION OUTLINE

The rest of the thesis is organized as follows. Background on related research is given in the Chapter 2. Chapter 3 describes the biometric analysis system developed for Nursebot. In that chapter, we introduce Naive Bayes model, the Gaussian Mixture model, and other techniques that are used in the filtering of the non-subject data. The results of the filtering are presented at the end of Chapter 3. Chapter 4 provides a description of SenseWear®PRO body monitor, its sensors, and the data collected by BodyMedia. Then theoretical foundations of Support Vector Machines and Decision Trees are given. Those are followed by a detailed description of Wellness Monitoring algorithm and the results of its application to the data from SenseWear®PRO monitor. An ongoing project of assessment of balance impairment and its preliminary results are presented in the Chapter 5. Chapter 6 concludes this thesis by providing a summary of the results and emphasizing the original contributions of this dissertation.

2.0 BACKGROUND AND SURVEY OF RELATED WORK

This research is based on analysis of speech data, gait data, and data from a wearable body monitor. In this chapter, we review the work related to the above mentioned biometrics, multimodal biometric systems, and wearable computers. The details regarding the methods and results of our biometric analysis techniques are discussed in the following chapters.

2.1 MULTIMODAL BIOMETRICS

Contemporary biometric recognition systems are not perfect. Even though their performance still can be greatly improved, the noise level of sensors, as well as other limitations in data acquisition and feature extraction, such as intra-class variations, distinctiveness, and non-universality [12], create an upper bound to recognition accuracy of a single biometric analyzer. It was shown in [13, 14] that the performance can be improved by integrating multiple biometrics in one system.

All people exploit data fusion routinely in their daily lives. The human brain is one of the best *multimodal fusion systems* known to us [15]. It processes and integrates sensory information to perceive its environment. Human sensors acquire data on sight, smell, touch, hearing, and taste. Then the brain uses memory and prior knowledge to produce an integral representation of the environment from that data.

Information fusion is a broad subject that studies how data and information from multiple sources can be combined in order to generate a single score or to reach a decision. Some of the advantages of multimodal data fusion are error reduction and increased reliability. In [14] the combined system of two speech recognition experts and three face recognition experts

increased the person identification accuracy by 15%-27% compared with the recognition accuracy of each expert taken independently. [16] demonstrated that integration of face and gait recognition systems improved the recognition results by either modality alone. One of the biometric analysis systems described in this thesis is based on gait and voice data, thus, we provide an overview of the research on those biometrics in the next two sections.

2.2 GAIT ANALYSIS

Gait is an important behavioral characteristic that has been always used for diagnostic purposes in conventional medicine. People tend to develop a pathological gait as a result of a disease, an injury, or simply fatigue. *Clinical gait analysis* is devoted to the study and identification of gait pathologies and malfunctions [17]. Data acquisition for clinical gait analysis is usually performed in a controlled environment under professional supervision using wearable devices [18], markers [19], or ground reaction force measurement platforms [20].

Psychological studies [21] have shown that gait is a unique characteristic of a person; and in the 90's gait emerged as a biometrics in person recognition research [22]. Today, automatic gait recognition is performed from image sequences of walking subjects. Currently there are two main approaches to video-based gait recognition: holistic [23, 24, 25] and model-based [26, 27, 28, 29].

The holistic, or model free, technique is purely an image recognition approach, in which the system analyzes all of the images of the walking person and extracts statistical information that is invariant for the same person, but disparate for different people. This method characterizes image patterns with no consideration to their underlying structure.

The aim of the model-based approach is to construct a biomechanical model of human motion, and then fit that model into image data. In [26] the gait signature is extracted from the images using the Fourier series to describe the motion of thighs and apply temporal techniques in order to extract the moving model from a sequence of images. While [29] uses a three dimensional human model to track and analyze the motion of each body part.

Some of the drawbacks of video-based gait analysis systems are that they usually depend on view, distance, background, clothing and shoes. The passive biometric monitoring system, that is the primary goal of this research, is going to be mounted on the nursebot. Thus, we cannot afford a view-dependent approach in our system, nor we can guarantee a distance of 15 feet or more to the subject, since the nursebot will be placed in an apartment or an eldercare institution. That is why we have taken a novel approach of gait analysis using audio and vibration signals of the foot impact with the floor.

2.3   SPEECH ANALYSIS

Automatic speech processing research started in the early 50's of the last century, when Bell Labs developed a speech recognition system that successfully identified the digits 0-9 spoken to it [30]. One of the problems of early voice analysis systems was that they were speaker dependent. Major developments in the speech recognition followed, and in the 70's some scientists looked into the related problem of *speaker* recognition by voice [31]. Today, speaker recognition applications have been successfully used for authentication, surveillance and law enforcement [32, 33].

How do we recognize people when they speak? Speech conveys several levels of information to us. At a low level (acoustic), we recognize a person's voice, i.e. vocal utterances, pitch, and nasality. At a middle level (phonetic), we hear the pronunciation of sounds and words, thus, we feel the accent and intonation. Finally, on a high level (linguistic) we recognize the speaker's linguistic style, vocabulary, mood, and speed of speech.

One of the goals in the nursebot project is to recognize the voice of the target subject, so that it can be analyzed for subtle changes that may characterize a person's overall wellness. Speaker recognition systems are characterized as either text-dependent or text-independent. Text-dependent systems rely on the restriction that the input phrase or sentence is the same during training and recognition phases of the system. Those systems are generally more robust, since the recognition is based on both the speaker's voice and the lexical content of the speech.

9

In our system, however, we are dealing with text-independent verification problem. Most of modern text-independent speaker recognition systems are based on one of the three principal models. These are vector quantization, statistical, and neural network models.

- The Vector Quantization (VQ) technique uses speaker-specific codebooks for classification purposes [34, 35]. These codebooks are constructed from the means of feature vector clusters during the training phase. Each cluster represents an acoustic unit for the target speaker. The recognition is performed by computing the quantization error between the test feature vector and the codebooks in the database. It was shown in [36, 37] that statistical models perform at least as good as or better than VQ-based model when sufficient data is available.

- The idea behind statistical methods is to compute the likelihood of the feature vector given the speaker model [36, 38]. The speaker model is based on the conditional probability density function constructed from the training set of feature vectors. For each speech frame, one can compute the feature vector and estimate the probability that it belongs to the claimed speaker. Multivariate normal density functions are often used to model speakers because of their simple parametric representation and ability to approximate real-world density functions. The speaker analyzer in our system is based on a statistical model, namely the Gaussian Mixture Model.

- A Neural Network model is a supervised learning approach to the speaker recognition problem [39, 40]. Typically, the neural classifier is trained to model the decision function which discriminates speakers; therefore, there is no need to build models for specific speakers. The network is trained to recognize the target person by activating the output units associated with that person and leaving the rest of the output units inactive. A major drawback of neural network models is the high computational cost of augmenting the training data, which makes it less practical for use in interactive systems.

2.4   WEARABLE COMPUTING

Since prehistoric times, humans have constantly tried to enhance their abilities by inventing tools. Computers brought that desire for personal empowerment to a whole new level by becoming tools that enhance not only the physical but also the mental abilities of humans. Nowadays, millions of people carry with them mobile computing devices such as wireless phones, personal data assistants, and multimedia players.

A wearable computer is a body-worn computing device that is always on and always ready and accessible. Steve Mann [41] became the pioneer of modern wearable computing in 1981 by inventing a wearable device that allowed him to control a camera and other photographic equipment. Since then advances in computer technology opened numerous opportunities for scientific and commercial applications of wearable computers in many fields. Some of the applications include wearable personal computers, aircraft maintenance assistants, remote sensing devices, and interactive navigation assistants.

Analog wearable devices for monitoring patient's health in ambulatory conditions were introduced several decades ago. The Holter monitor, the first ambulatory electrocardiographic recorder, was introduced in 1961 [42]. It was worn by a patient for about 24-48 hours to obtain a continuous recording of heart rhythm during normal activity. There has been tremendous progress in the ambulatory patient monitoring in the last decade with the invention of wearable computing devices that continuously collect data on person's vital signs, pulse, movements, sleep, and brain activity.

One of the most innovative and unobtrusive approaches to biomonitoring is the ring sensor developed at MIT [43]. The device is worn on a finger as an ordinary ring, and it employs pulse oximetry methods to acquire heart rate and oxygen saturation data necessary for assessment of the patient's cardiovascular state. The ring sensor uses its low power transceiver for uploading the data to the base station and for reconfiguration without removing the biosensor from the patient's finger.

There are a number of researchers working on "smart" clothing solutions. These garments monitor health and wellness of people using embedded microsensors. The wearable motherboard is a textile engineering project at Georgia Tech, which introduced a notion

of wearable integrated information structure [44]. The flexible data bus embedded in the material transmits biometric signals such as temperature and heart rate to the monitoring devices. The results of this research were implemented in a commercial product SmartShirt® by Sensatex. Philips Research [45] ad VivoMetrics [46] have taken analogous approaches to health monitoring using biomedical clothing.

SenseWear®PRO by BodyMedia is another successful commercial product, that is arguably more practical in continuous wellness monitoring [4]. SenseWear®PRO is an armband that uses 2-axis accelerometer, two temperature sensors, galvanic skin response sensor, and heat flux sensor to collect physiological data. By combining the movement data from the accelerometer with the data from the other biometric sensors SenseWear®PRO dynamically identifies person's physiological and activity context at the current moment [47]. Using context-specific algorithms with the acquired data BodyMedia obtained an accurate estimate of energy expenditure while performing that specific activity [48]. What is remarkable about SenseWear®PRO that it can perform those tasks in unsupervised mode, and it can go for three days without a recharge. Therefore, it allows the most flexibility and convenience to the person who wears it.

3.0   NON-INTRUSIVE BIOMETRIC ANALYSIS

This chapter describes the implementation of the non-intrusive multimodal biometric monitoring system for the nursebot and the results of testing of its capability to filter out the data collected from non-target subjects. The overall design of the system is shown on Figure 1.

The system collects data about the subjects' gait and voice using three channels: two audio channels and one vibration channel. One of the audio channels and the vibration channel are used for gait analysis. The other audio channel is used for voice analysis. The raw data from each channel is preprocessed with Fourier transforms.

Gait analysis in our biometric system is performed from audio and vibration signals of footfalls. This is a novel approach in gait analysis, as previous work in automatic non-intrusive gait analysis is concentrated on video-based methods that were discussed above. The data is processed and classified using Naive Bayes Model [49] for audio and vibration channels independently. Information fusion of the data from the both channels is performed on the decision level using adaptive weighted sum approach.

Dimensionality of gait channels is reduced with principal component analysis. Then two Naive Bayes classifiers are applied to the features for each gait channel separately, and the log output of discriminant functions of those classifiers is supplied as an input to the adaptive data fusion system based on a single sigmoidal unit.

We have chosen a statistical approach for voice analysis and speaker recognition in our system. Namely, we use the Gaussian Mixture Model to model the voice of the target subject. As it was mentioned previously, statistical methods are more accurate than the VQ-approach and require less computational power for training than neural network models. We use mel-frequency cepstrum coefficients obtained from the time-frequency representation
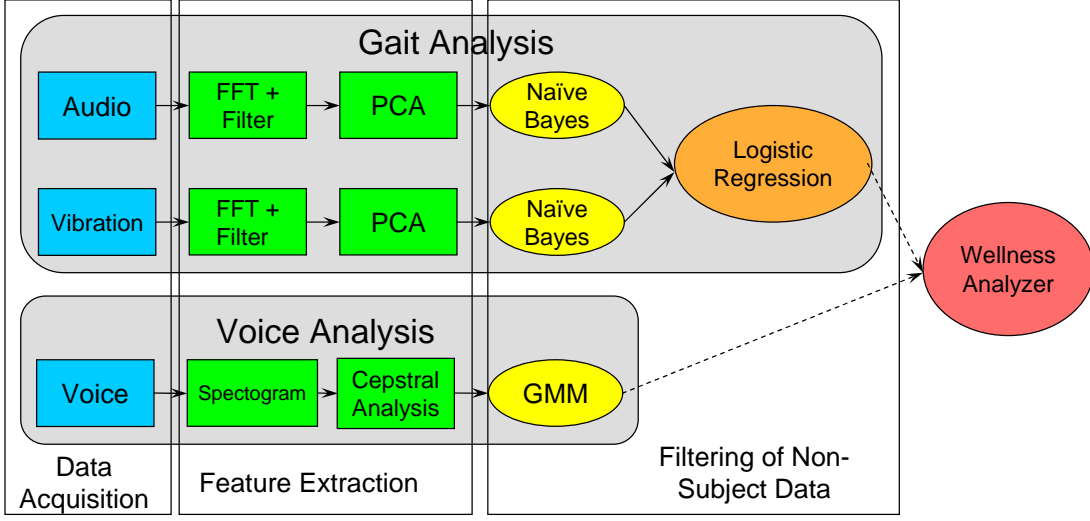
Figure 1: Multimodal biometric monitoring system

of the speech data as our features for the mixture model. It was shown in [50, 51] that cepstrum provides the best results for speaker recognition compared to linear prediction (LPC), impulse response, autocorrelation, vocal tract area function, and pitch.

The temporal characteristics of speech are preserved in the feature space by applying a sliding window to the raw data prior to spectral analysis, which produces a spectogram, a time-frequency representation of audio data. Voice features are obtained by applying mel-scaled filterbank to spectogram data. Then discrete cosine transform is used for dimensionality reduction of voice features. Finally Gaussian Mixture Model is used for classification of mel-cepstrum features obtained in above-mentioned steps.

The next section provides the details about the methods used for the gait analysis in the biometric monitoring system. The description of the feature extraction and classification techniques for the voice analysis are given in Section 3.2. The testing results of the system are presented in Section 3.3.

3.1 GAIT ANALYSIS

3.1.1 Signal Processing

We begin by building a system that analyzes data collected from a piezoelectronic accelerometer and a microphone at sampling rate of 20KHz (Figure 2).
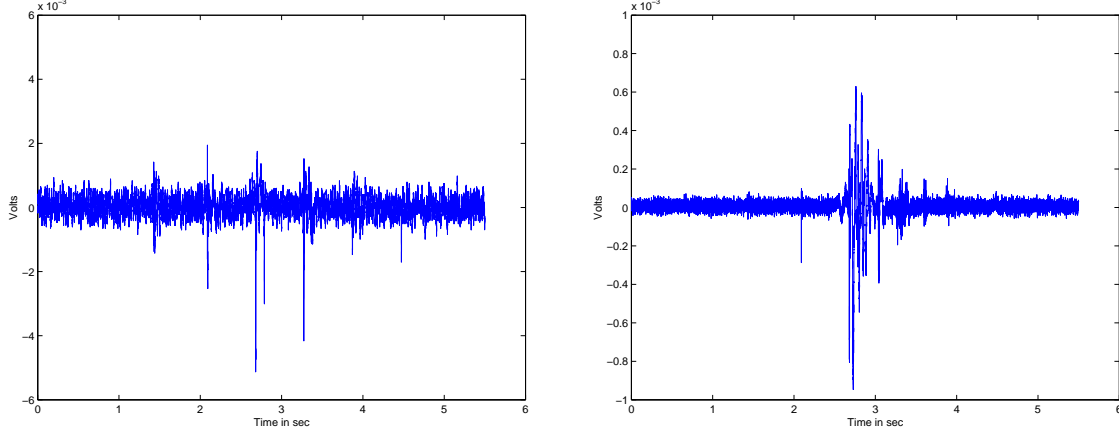
Figure 2: Unprocessed signals from the accelerometer (left) and the microphone

The most significant footstep for each pair of "raw" signals is extracted by detecting the largest peak and taking $N = 10000$ data points in its neighborhood. Further processing is done in spectral domain. We take discrete Fourier Transform of the signal $\mathbf{x}$

$$X(k) = \sum_{n=0}^{N-1} x(n) e^{-i \frac{2\pi}{N} nk}. \tag{3.1}$$

Then we use an ideal lowpass filter on $\mathbf{X}$ with a cutoff frequency of 4KHz. The resulting filtered spectrum is shown on Figure 3.

3.1.2 Feature Extraction

In order to make sense of our data we need to reduce the number of dimensions, since it would be computationally hard to work with 2000 features per sample. One of the widely used dimensionality reduction methods is Principal Component Analysis (PCA). PCA performs linear transformation that aligns the transformed axis with the directions of maximum

15

variance. Basis vectors in those directions are called *principal components* . Principal components are known to be eigenvectors of the covariance matrix of samples, taken in decreasing order of corresponding eigenvalues [52], i. e. the first principal component is an eigenvector
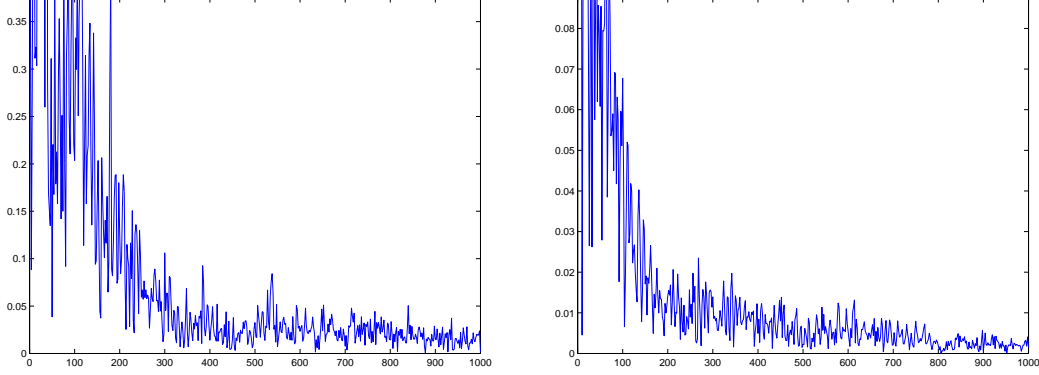
Figure 3: Fragment of filtered spectrum of signals from accelerometer (left) and microphone

corresponding to the largest eigenvalue of the (sample) covariance matrix. Alternatively k-th principal component can be recursively expressed through the previous $k-1$ components as

$$\mathbf{w}_k = \arg\max_{|w|=1} E\left(\left(\mathbf{w}^{\mathrm{T}}\left(\mathbf{x} - \sum_{i=1}^{k-1} \mathbf{w}_i \mathbf{w}_i^{\mathrm{T}} \mathbf{x}\right)\right)^2\right).\tag{3.2}$$

The first few dimensions of PCA transformed data contain most of information about the data. Therefore, we keep the first 30 features for each of the samples as our main features for classification purposes.

3.1.3   Naive Bayes Model

We use Naive Bayes Model in order to separate the main subject from the rest. Let ω_1 be the state that the sample was collected from the main subject, and ω_2 be the state that the sample was collected from another subject. Let $P(\omega_i)$ be the *a priori* probability that the nature is in state ω_i. Then we compute the posterior probability $P(\omega_i|\mathbf{x})$ using Bayes rule

$$P(\omega_i|\mathbf{x}) = \frac{p(\mathbf{x}|\omega_i)P(\omega_i)}{p(\mathbf{x})},\tag{3.3}$$

where x is a feature vector, and

$$p(\mathbf{x}) = p(\mathbf{x}|\omega_1)P(\omega_1) + p(\mathbf{x}|\omega_2)P(\omega_2)$$

16

and $p(\mathbf{x}|\omega_i)$ is a state conditional probability density function. Since the denominator for both $P(\omega_i|\mathbf{x})$ is the same, we take logarithms of numerators as our discriminant functions

$$g_i(\mathbf{x}) = \log p(\mathbf{x}|\omega_i) + \log P(\omega_i). \tag{3.4}$$

Our classifier can be viewed as a machine that selects the category which has the larger discriminant.

A multivariate normal density has been chosen for the conditional density function $p(\mathbf{x}|\omega_i)$. Our data features are real valued, and we expect them to be slightly skewed versions of the prototype vector $\boldsymbol{\mu}_i$, therefore, normal density is an appropriate model for our case [2]. In addition we make the *naive* assumption that our features are independent given the class, thus

$$p(\mathbf{x}|\omega_i) = p(x_1|\omega_i)p(x_2|\omega_i)\dots p(x_n|\omega_i). \tag{3.5}$$

We apply the maximum likelihood principle and use the training samples $D = \{D^1, \dots, D^K\}$ to estimate parameters for density functions for each feature in each class.

$$L(D_j, \mu_j, \sigma_j) = \log \prod_{k=1}^{K} p(x_j^k|\mu_j, \sigma_j) = \sum_{k=1}^{K} p(x_j^k|\mu_j, \sigma_j), j = 1, \dots, n. \tag{3.6}$$

Thus, we obtain maximum likelihood estimates of means and variances:

$$\hat{\mu}_j = \frac{1}{n}\sum_{k=1}^{K} x_j^k \quad \hat{\sigma}_j = \frac{1}{n}\sum_{k=1}^{K}(x_j^k - \hat{\mu}_j)^2. \tag{3.7}$$

3.1.4 Fusion of Audio and Vibration

All of the above mentioned data processing and modeling have been done for samples from each channel (vibration from accelerometer and audio from microphone) independently from the other channel. Next, the data collected from different sensors is combined in order to improve the model of the patient's condition.

We have constructed a logistic regression model for the fusion of vibration and audio data characterizing the gait. The values of discriminant functions from Bayes model for audio and vibration signals are supplied as 4 inputs to a single sigmoidal unit

$$\mathbf{a} = (g_{1v}(\mathbf{x}_v), g_{2v}(\mathbf{x}_v), g_{1a}(\mathbf{x}_a), g_{2a}(\mathbf{x}_a)). \tag{3.8}$$

We make the decision by rounding the sigmoidal probabilistic function:

$$p(y = 1|\mathbf{a}, \mathbf{w}) = f(\mathbf{a}, \mathbf{w}) = \frac{1}{1 + e^{-\mathbf{w}^{\mathrm{T}}\mathbf{a}}}, \tag{3.9}$$

where $\mathbf{w}$ is a set of weights found in the training stage, and the output $y = 1$ indicates the target subject.

We proceed with maximum likelihood estimation for parameter learning.

$$L(D, \mathbf{w}) = \log \prod_{k=1}^{K} p(y = y_k|\mathbf{a}, \mathbf{w}) = \sum_{k=1}^{K} f(\mathbf{a}, \mathbf{w})^{y_k}(1 - f(\mathbf{a}, \mathbf{w}))^{(1-y_k)} \tag{3.10}$$

We maximize the log-likelihood of the output using online gradient decent algorithm [53]:

$$\mathbf{w}_{k+1} = \mathbf{w}_k + \rho_k(y_k - f(\mathbf{w}_k, \mathbf{a}_k))\mathbf{a}_k. \tag{3.11}$$

3.2 VOICE ANALYSIS

3.2.1 Cepstral Feature Extraction

Feature extraction for voice analysis follows that described in [36]. Speech spectrum is one of the best known characteristics of a speaker [31]. Therefore, we proceed with frame-based spectral analysis. We have obtained the spectrogram $X_m(n)$ of the speech signal $\mathbf{s}$ by taking the short-time Fourier Transform with a Hamming window of length 25.6 ms ($N = 512$)

$$X_m(k) = \sum_{n=0}^{N-1} x_m(n)e^{-i\frac{2\pi}{N}kn}, \tag{3.12}$$

where $x_m(n) = Ham(n)s(n - mT)$ and m is the frame number.

Next we apply *mel-scaled* filterbank of 29 overlapping triangular filters $F(j,k)$ to the spectogram magnitude

$$S_m(j) = \sum_{k=0}^{N-1} F(j,k)|X_m(k)|. \tag{3.13}$$
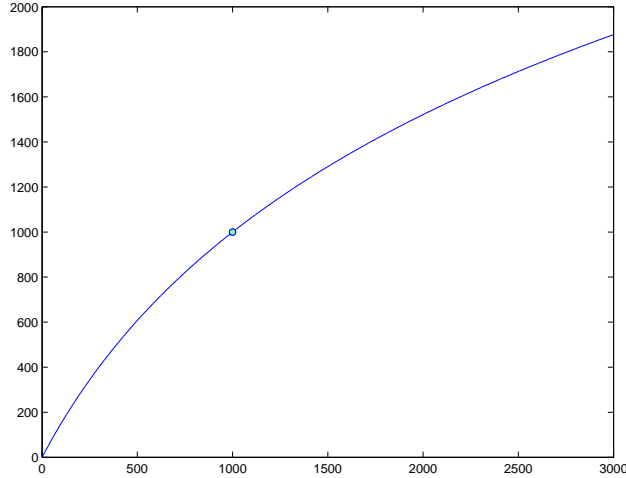
Figure 4: Mel frequency scale is used for modeling of the human perception of sound

Mel frequency scale is based on human perception of the frequency content of sounds [54]. It is approximately linear below 1000 Hz and logarithmic above as shown on Figure 4:

$$Mel(f) = 1127\log(1 + \frac{f}{700}). \tag{3.14}$$

We obtain the cepstral coefficients $c_m(n)$ by taking the discrete cosine transform of the logarithm of the filterbank output.

$$c_m(k) = \sum_{j=0}^{J-1} \log(S_m(j)) \cos\left(\frac{\pi(2j+1)k}{2J}\right).$$
(3.15)

Cosine transform helps to decorrelate the data, and thus, reduces its dimensionality.

Finally, we form our feature vector from 12 cepstral coefficients, beginning with the second one. This process is repeated every 12.8 ms, producing about 78 feature vectors per second.

3.2.2 Gaussian Mixture Model

Human speech is a complex audio signal, and due to phonetic diversity it would be extremely hard if not impossible to come up with a simple parametric density model that effectively characterizes the speaker. So it is natural to describe it as a mixture of several density of functions. Gaussian Mixture Model was shown to be quite successful in solving speaker and speech recognition tasks [36, 38].

The probability density function of the Gaussian mixture is given by

$$p(\mathbf{x}|\theta) = \sum_{m=1}^{M} w_m \mathcal{N}(\mathbf{x}|\boldsymbol{\mu}_m, \Sigma_m),$$
(3.16)

where $\mathbf{x}$ is a feature vector and $\theta = \{w_m, \boldsymbol{\mu}_m, \Sigma_m\}, m = 1, \ldots, M$. w_m's represent prior probabilities for each class, and they are called *mixing parameters* or *weights*. Conditional densities $\mathcal{N}(\mathbf{x}|\boldsymbol{\mu}_m, \Sigma_m)$ are called *component densities*, and in our case, they are $d-$variate Gaussians of the form

$$\mathcal{N}(\mathbf{x}|\boldsymbol{\mu}_m, \Sigma_m) = \frac{1}{\sqrt{(2\pi)^d|\Sigma_m|}} e^{-\frac{1}{2}(\mathbf{x}-\boldsymbol{\mu}_m)^{\mathrm{T}}\Sigma_m^{-1}(\mathbf{x}-\boldsymbol{\mu}_m)}.$$
(3.17)

We use the training data for the target speaker to estimate the mean vectors, weights, and component densities for his/her model θ. In our model each Gaussian component has

a diagonal covariance matrix. We proceed with parameter estimation using the Maximum Likelihood principle:

$$L(\mathbf{X}|\theta) = \prod_{k=1}^{K} p(\mathbf{x}_k|\theta), \tag{3.18}$$

where $\mathbf{X} = \{\mathbf{x}_1, \ldots, \mathbf{x}_K\}$ is a set of K training vectors. Direct estimation of parameters θ is not possible due to their nonlinearity. Therefore, we apply an iterative estimation method known as Expectation Maximization (EM) algorithm [55].
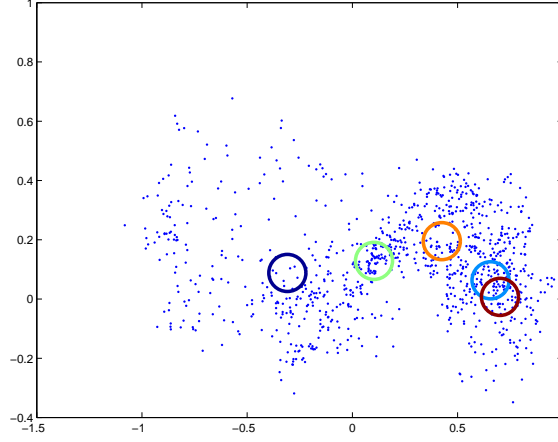
Figure 5: The graph depicts two out of 12 dimensions from the database of cepstral coefficients of a single person. 5 colored circles are centered in the means of 5 component densities of the Gaussian mixture which models that person's voice.

During the *E-step* of the algorithm, we compute posterior probabilities for each class ω_i using Bayes rule

$$P(\omega_i|\mathbf{x}_k, \theta(j)) \quad = \quad \frac{p(\mathbf{x}_k|\omega_i, \theta(j))P(\omega_i|\theta(j))}{p(\mathbf{x}_k|\theta(j))} \quad = \quad \frac{\mathcal{N}(\mathbf{x}_k|\boldsymbol{\mu}_i(j), \Sigma_i(j))w_i(j)}{\displaystyle\sum_{m=1}^{M}\mathcal{N}(\mathbf{x}_k|\boldsymbol{\mu}_m(j), \Sigma_m(j))}. \tag{3.19}$$

We obtain local-maximum-likelihood estimates of the parameter values during the *M-step*

$$\boldsymbol{\mu}_i(j+1) = \frac{\displaystyle\sum_{k=1}^{K} P(\omega_i|\mathbf{x}_k, \theta(j))\mathbf{x}_k}{\displaystyle\sum_{k=1}^{K} P(\omega_i|\mathbf{x}_k, \theta(j))}, \tag{3.20}$$

$$\Sigma_i(j+1) = \frac{\displaystyle\sum_{k=1}^{K} P(\omega_i|\mathbf{x}_k, \theta(j))(\mathbf{x}_k - \boldsymbol{\mu}_i(j+1))(\mathbf{x}_k - \boldsymbol{\mu}_i(j+1))^{\mathrm{T}}}{\displaystyle\sum_{k=1}^{K} P(\omega_i|\mathbf{x}_k, \theta(j))}, \tag{3.21}$$

$$w_i(j+1) = \frac{1}{K}\sum_{k=1}^{K} P(\omega_i|\mathbf{x}_k, \theta(j)). \tag{3.22}$$

Figure 5 illustrates the centers of clusters where the means of five Gaussians that form the mixture for the target subject are located.

Classification of speakers into target and impostor subjects is done using Bayes rule (3.3) and the discriminant function (3.4). The discriminant function in this case compares the posterior probabilities of the mixture model for the target person with the mixture model for the rest of the subjects.

3.3 RESULTS

3.3.1 Gait Analysis

We have conducted our gait analysis experiments on 260 recordings of data from 22 subjects. There have been 50 audio and vibration recordings collected from the target subject in 50 sessions. We have recorded 10 sessions of data from each of the other 21 subjects.

As it was mentioned in Subsection 3.1.1, only the data corresponding to the most significant footstep is extracted from each session recording for further processing and classification tasks. That data is obtained by taking a window of data points in the neighborhood of the

largest peak. We have analyzed the false-accept rate and total misclassification error depending on the window length (Figure 6). It can be seen on the graphs that the total misclassification error does not change significantly for window lengths of 5000 to 10000. However, the false-accept rate exhibits some decreasing trend as the window length increases.
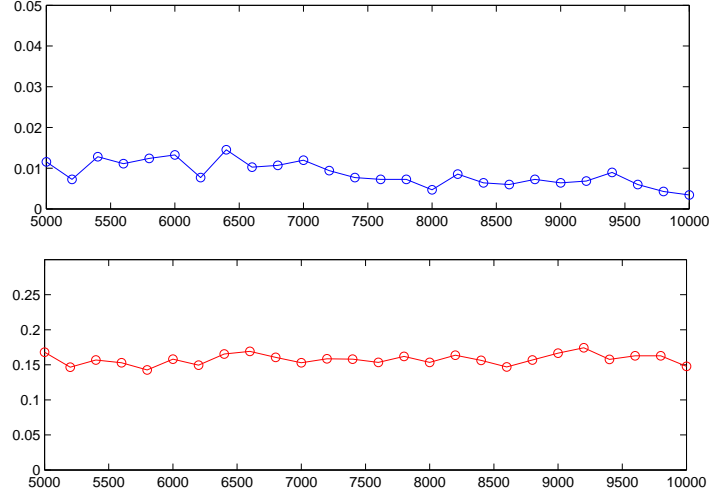
Figure 6: False-positive rate (upper) and total misclassification error (lower) based on window length

We have also observed that the signal to noise ratio decreased as the window length increased. Therefore, based on signal to noise and classification analysis of window length we have set the length of our window of interest at $N = 10000$. The mean signal to noise ratio averaged over the window of interest is equal 2.49 dB for vibration signal and 5.67 dB for audio signal.

The goal of our experiments is to reliably identify the target subject data from the rest of the data, using the binary classification model described in Section 3.1.4. Following the terminology of biometric recognition literature, the two classes, separated by our binary classifier, are called the genuine and the impostor classes. The genuine class in our system consists of the target subject data. The impostor model in out system is based on the data from all other subjects. We have made preliminary statistical analysis of the data in order to justify the choice of the impostor model. We performed PCA on 50 samples from the target subject and on 50 samples from five non-target subjects. As it can be seen from Figure 7, the standard deviation of each dimension in PCA transformed data is smaller for the impostor
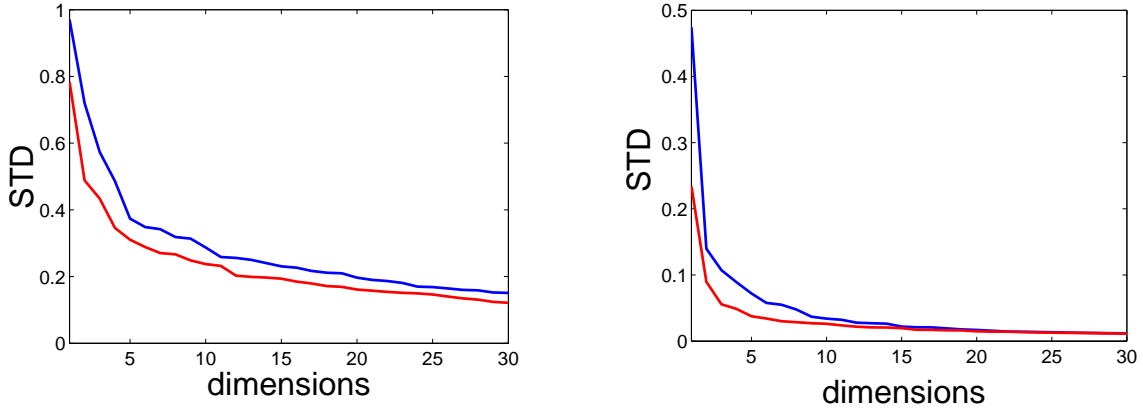
Figure 7: PCA analysis of impostor and target data. Vibration signal is on the left, audio signal is on the right. Red line is the standard deviation per dimension for the target subject, blue is the standard deviation per dimension for non-target subjects.

model than that for the genuine model. It implies that the collection of data from a group of subjects displays more variability than the data from a single subject. Therefore, our impostor model can be used for approximation of the universe of all people which are not the target subject.
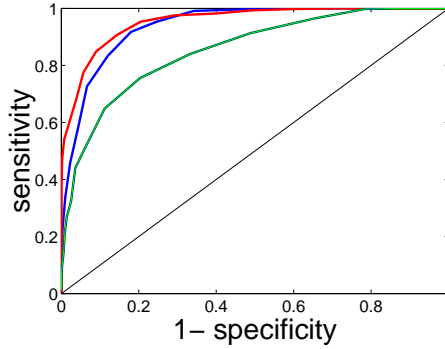
Figure 8: ROC curves: the red one is the integrated classifier, the blue one is the vibration channel only, and the green one is the audio channel

We could identify the target person by his/her gait with about 84% accuracy, using combined data from audio and vibration channels. The results of classification are often presented in a confusion matrix. The columns of that matrix depict the actual class mem-

bership, while the rows show the predicted class counts. For example, the upper right cell contains the false positive results. The averaged confusion matrix of a person authentication by gait based on 30 iterations, and 30%-70% split of the data into testing and training sets for each iteration is shown in Table 1.

A receiver operating characteristic (ROC) is a graphical plot of the true-accept rate vs. the false-accept rate for a binary classifier system as its discrimination threshold is varied. The true-accept rate is also called the classifier's sensitivity, and the false-reject rate is called its specificity. It is clear from the ROC curves shown in Fig. 8 that by integrating the channels we have improved recognition rates. We can tolerate high true-reject rate, since, in our specific case of strong verification problem we are mainly interested in low relative false-accept rate, which we define as the ratio of false-accepts to a total number of accepted samples. That is because we are conducting long term monitoring, thus, we have access to very large amount of subject data. Therefore, we can reject a lot of subject data as long as we keep some (in this case about one-fifth). However, we would like to include as few non-subject features in our training set as possible.

Table 1: Confusion matrix of gait recognition with integrated system of audio and vibration channels

		Actual	
		Target	Impostor
Prediction	Accept	4.44%	1.28%
	Reject	14.79%	79.49%

As it was mentioned in the previous chapter the classification of data is performed in two steps. Initially we use Naive Bayes analyzer, then its output is fed to a sigmoidal unit. The preliminary results show that the relative false-accept rate is 22.38% which is somewhat high. That can be explained by the relatively small amount of testing data, so that in this case only one $(0.0128 * 78 = 0.998)$ falsely accepted feature greatly impacts relative false accept rate. Therefore, we can expect the relative false-accept rate to drop significantly in experiments with a larger corpus of data. Finally, the overall accuracy and the false-accept rate can be further improved by integrating the gait subsystem with the substantially more accurate

voice subsystem, the experimental results of which are presented in the next subsection.
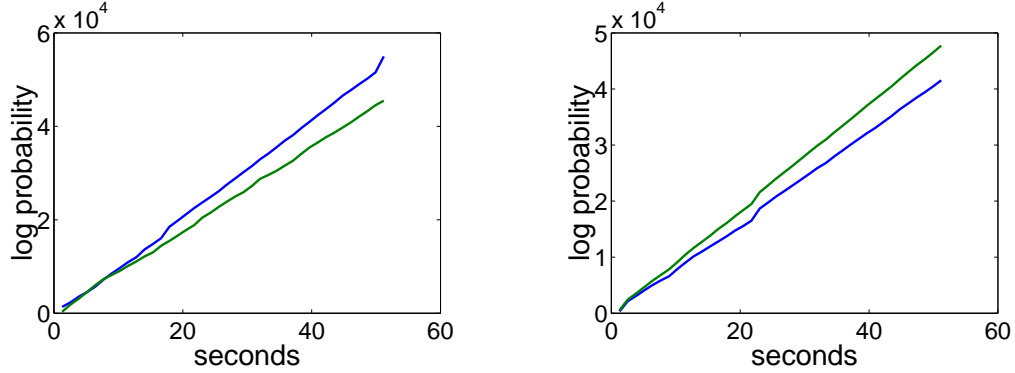
Figure 9: Posterior probabilities of the target subject's test data (left) and impostor's test data (right) computed with target subject's model (blue) and the impostor model (green).

3.3.2   Voice Analysis

Voice recognition was performed on speech data collected from 7 people. Each recording is about 1 minute long. We used 10 seconds of each recording for training purposes, and we tested our model on the remaining parts.

It can be seen from the graph (Figure 9) that we are able to verify our target subject with about 10 seconds of speech data. As it was expected, the longer speech sample we are given the more reliable is the authentication. The speech was recorded in a relatively noise-free environment. Because of the low number of subjects and the controlled conditions, person identification using Gaussian Mixture Model was near perfect (over 98% accuracy).

We used a mixture of five Gaussians in our subject model. Table 2 shows the means of multivariate components of the mixture for the target model. Figure 10 shows the projections of the target and impostor mixture models into 3D space.

In general the accuracy results deteriorate with the number of people in the environment and the background noise. However, in an eldercare environment, the universe of individuals likely to come in contact with the subject is limited, typically consisting of family members and a small population of caregivers. Therefore, good accuracy results in our experiments are likely to be reproduced in real-world settings.

Table 2: Means of the mixture model for the target subject

Components	1	2	3	4	5
Weights	0.0886	0.1411	0.2457	0.4407	0.0836
Dimensions	-0.6615	0.4551	-0.1068	0.6385	0.0838
	0.4372	0.1794	0.0476	-0.0205	0.0753
	0.1171	0.18687	0.1949	0.1315	0.0716
	-0.0423	0.1565	0.0613	0.0185	0.0998
	0.1480	0.0095	-0.0093	-0.1753	0.0257
	-0.1440	-0.1124	-0.0314	-0.0429	-0.1140
	-0.0586	-0.0009	-0.0241	-0.0184	-0.0015
	0.0839	-0.0050	0.0441	-0.0790	0.0491
	-0.0106	-0.0115	0.0460	0.0117	0.1023
	0.0108	-0.0790	-0.0098	0.0091	-0.0429
	-0.0207	-0.0423	-0.0009	-0.0242	-0.0410
	0.0442	0.03724	0.0338	0.0392	0.1029
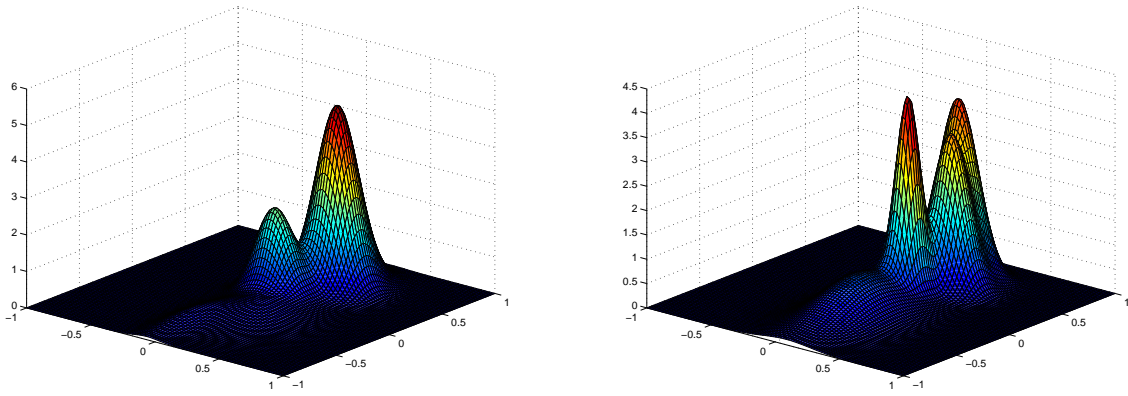
Figure 10: Projections of twelve-dimensional mixtures of Gaussians into 3D space. The target model is on the left, and the impostor model is on the right.

4.0   BIOMETRIC MONITORING WITH A WEARABLE DEVICE

This chapter describes the wellness monitoring algorithm that can be applied to any system that is based on a subject model based on binary classification of the feature vectors. Thus, the algorithm can be applied to the biometric analysis system and the subject model previously described in the Chapter 2. However, in this chapter, we report the methods and results of the application of the algorithm to the data collected using the SenseWear®PRO body monitor.

In the biometric analysis system that has been built for the nursebot project, binary pattern classification techniques were used to distinguish the target subject from the impostors. Specifically, the system separated the data, that corresponded to a normal gait of the target subject, into one class, and the rest of the data were put into another one. As an added bonus of that approach, the subject data, that was not normal gait such as running or jumping data, was classified as impostor data. If it were necessary to monitor other activities besides normal gait, additional classifiers would have to run in parallel to the main one.

Context-awareness is one of the central issues in wearable computing applications [56]. In the experimental setup involving the SenseWear®PRO armband the device is constantly worn by the subject, and thus, there is no need to verify the subject's identity. This setup provides substantially more data for analysis and allows monitoring of the subject's wellness at all times. However, the biometric readings of the person during sleep are substantially different from those in the course of exercising. Therefore, the wellness monitoring system based on the SenseWear®PRO body monitor has to be context-aware. In other words the system should be able to identify the subject's activity prior to making the decision on his/her wellness.

The wellness monitoring process consists of four phases which are shown in Figure 11.

After the initial preprocessing, data collected with SenseWear®PRO is supplied to a binary classifier which selects the data representing the target context. The target context data is supplied to the wellness monitoring module which builds a new subject model. The new model is then used to assess the current condition of the subject using the past data for the target context.

Experimental data was obtained from BodyMedia in the form of nine channels of one-minute aggregate features. Support Vector Machines, Naive Bayes, and Decision Tree classifiers have been applied to the data for context recognition purposes. Support Vector Machines has been selected as a binary classifier for implementing the monitoring algorithm based on its performance in context recognition. It has been trained and tested on sleeping activity as the target context, since the number of available sample vectors representing that activity was substantially larger than the number of samples for any other single activity.
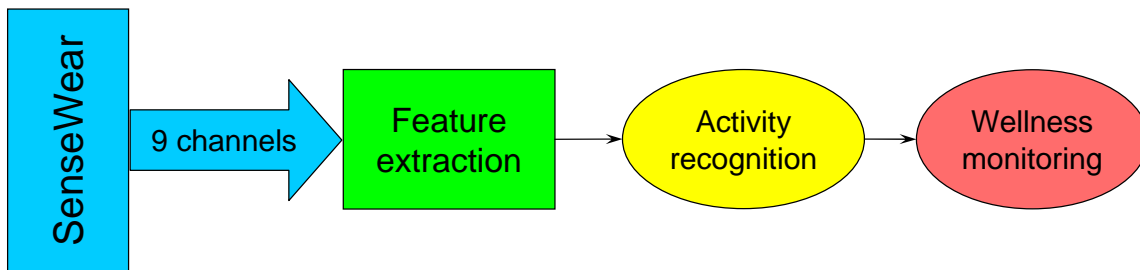
Figure 11: Wellness monitoring system based on SenseWear®PRO body monitor

The description of the SenseWear®PRO biometric monitoring device and its sensors is given in Section 4.1. Section 4.2.1 and 4.2.2 provide the details on Support Vector Machines and Decision Tree classifiers correspondingly. Naive Bayes classifier has already been described in Subsection 3.1.3 of Chapter 3. Section 4.3 explains the wellness monitoring algorithm. The experimental setup and results are presented in Section 4.4.

4.1   SENSORS OF THE BIOMETRIC MONITOR

Physiological and motion data for wellness monitoring was recorded with SenseWear®PRO armband from BodyMedia [4]. There are five sensors embedded in the armband: 2-axis accelerometer, heat flux sensor, galvanic skin response sensor, thermometer of skin temper-

ature, and thermometer of near body temperature. SenseWear®PRO is worn on the back of the upper arm as shown on the Figure 12. The description of the sensors is given below.

Figure 12: Wearable biometric monitor SenseWear®PRO worn on the upper arm of a subject

The accelerometer mounted on SenseWear®PRO is an inertial sensor that measures the component of translational acceleration minus the component of gravitational acceleration along 2 orthogonal axes. When the person is standing up with arms down to his sides, the transverse axis is oriented straight through the chest and parallel to the ground. Thus, the transverse component of the accelerometer provides information on horizontal motion by measuring the translational acceleration. The longitudinal axis is oriented parallel to person's body. The longitudinal component of the accelerometer obtains orientation information by detecting changes in the projection of the static gravitational acceleration.

The heat dissipation of the body is measured with a proprietary heat flux sensor. It consists of a plate with a sensitive thermocouple array between the top and bottom. Each thermocouple generates voltage proportional to the temperature difference between its joints. The sensor is made of materials with low thermoresistance so that the thermal flow disturbances are reduced to minimum. Its one side touches the skin and the other is exposed to the environment in order to facilitate thermal conduction.

Galvanic skin response (GSR) sensor measures skin conductance between two hypoallergenic stainless steel electrodes integrated into the underside of the armband. Skin conductance is a function of the sweat gland activity and the skin's pore size. Thus, changes in skin conductance are triggered by sweating either from physical activity or emotional

Table 3: List of preprocessed channels of data

Channel	Name	Description	Unit
1	GSR Mean	Skin conductance	micro Siemens
2	Heat Flux Mean	Heat loss of the body	Watts/meter^2
3	Near Body Temp Mean	Temperature near armband	Celsius
4	Pedometer	Number of steps	steps
5	Skin Temp Mean	Temperature of skin	Celsius
6	Long. Accelerometer SAD	Sum of absolute differences of vertical acceleration	g
7	Long. Accelerometer Mean	Mean vertical acceleration	g
8	Trans. Accelerometer SAD	Sum of absolute differences of horizontal acceleration	g
9	Trans. Accelerometer Mean	Mean horizontal acceleration	g

stimuli. In addition, the sweat rates determined from skin conductance convey important information about evaporative heat loss.

SenseWear®PRO is equipped with two thermistor based sensors. Thermistors are temperature dependent semiconductor resistors. One of them is located on the back of the armband and is in contact with the skin. It measures the skin temperature, which is correlated with the core temperature of the body. The other thermometer is placed on the side of the armband and measures the near-body ambient temperature. It provides information about environmental conditions around the armband.

SenseWear®PRO monitor can collect and store data up to five days without recharging. It is equipped with a wireless transmitter to allow for real time monitoring. All sensors collect data at constant sampling rate of 32Hz. The device then preprocesses the data and stores nine aggregate features (means, absolute differences, etc) per minute. Thus, the effective feature sampling rate is one sample per minute. Table 3 lists all channels with their respective interpretation. A typical output of the channels is shown in Figure 13.

Due to the aggregate nature and a low sampling rate of the data obtained from the
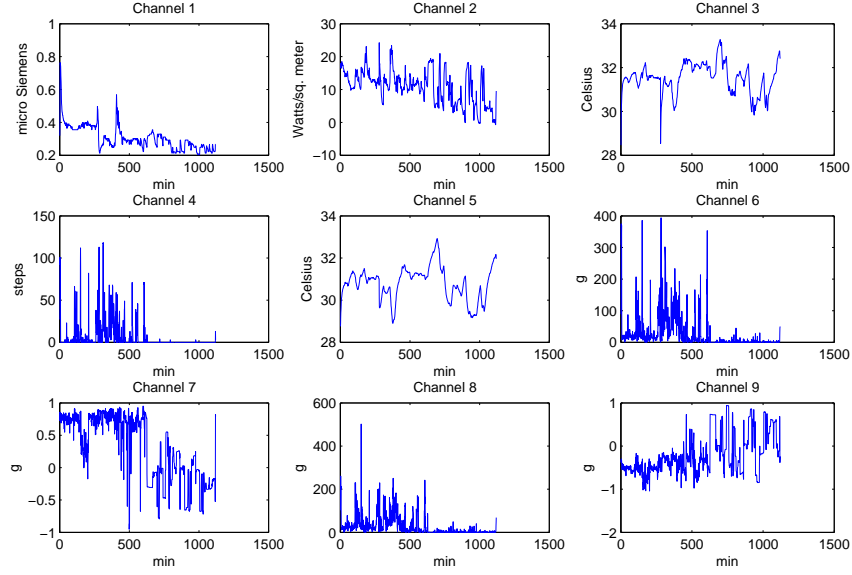
Figure 13: Typical outputs of the aggregate channels of SenseWear®PRO

SenseWear®PRO, most of feature extraction techniques have had either limited or no effect on the results. Thus, we have used *feature selection* methods which either preserve or entirely drop each of the channels from the feature set depending on their impact on the classification accuracy. The details about those methods are discussed in Subsection 4.4.1. Meanwhile, the next section describes the binary classification methods used for activity recognition.

4.2 ACTIVITY RECOGNITION

The context-awareness is a desirable property of any wearable computing device [57]. In the wellness monitoring problem, a person's physiological and behavioral traits when s/he is running can be substantially different from those when the person is sleeping. Thus, it is imperative to compare only homogeneous data in order to assess person's overall condition objectively.

We have compared three binary classification methods in their ability to identify the context activity in the data collected with the SenseWear®PRO. The description of Support

Vector Machines and Decision Trees is presented in this section. Naive Bayes Model is described in Subsection 3.1.3 of Chapter 3.

4.2.1 Support Vector Machines

Binary Support Vector classification is based on optimal hyperplanes that separate feature vectors [58, 59]. Let $\{\mathbf{x}_i\}, i = 1, \ldots, n$, be the training data and $\{y_i\}$ their corresponding labels, where $\mathbf{x}_i$-s are feature vectors, and y_i-s are either +1 for the target class or -1 for the impostor class. At first we assume that the data is linearly separable. Namely, there exists a hyperplane which separates the data according to their classes. This hyperplane H_s can be described by equation $\mathbf{x}^T\mathbf{w} + w_0 = 0$, where $\mathbf{w}$ is normal to the hyperplane. We define the margin of a separating hyperplane as the sum of distances from the hyperplane to the closest datapoints on each side. A separating hyperplane that maximizes the margin is called the optimal separating hyperplane (shown in Figure 14). Given a separating hyperplane H_s we can adjust $\mathbf{w}$ and w_0 so that the training data satisfy the following conditions:

$$\mathbf{x}_i^T\mathbf{w} + w_0 \geq +1, \text{ for } y_i = +1$$
$$\mathbf{x}_i^T\mathbf{w} + w_0 \leq -1, \text{ for } y_i = -1. \tag{4.1}$$
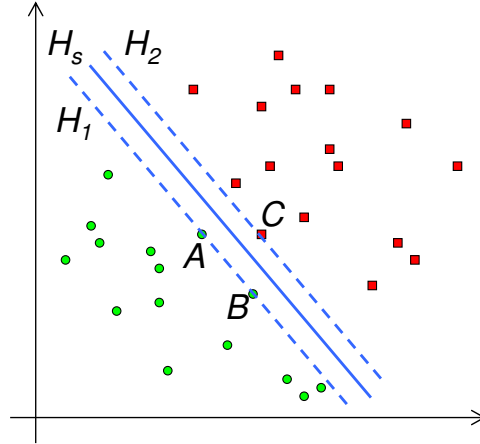
Figure 14: H_s is the optimal separating hyperplane; H_1 and H_2 are the canonical hyperplanes; A, B, and C are the support vectors.

Hyperplanes H_1 and H_2 defined by $\mathbf{x}^T\mathbf{w} + w_0 - 1 = 0$ and $\mathbf{x}^T\mathbf{w} + w_0 + 1 = 0$ are called canonical hyperplanes (shown in Figure 14). No feature vector lies between H_1 and H_2, and the vectors which lie on H_1 and H_2 are called support vectors (shown in Figure 14). Canonical hyperplanes are parallel to a corresponding optimal separating hyperplane H_s, and the margin of H_s is equal to the distance between H_1 and H_2. Therefore, the problem of finding an optimal separating hyperplane is reduced to maximizing $\frac{2}{\|\mathbf{w}\|}$, the distance between canonical hyperplanes. This can be formulated as a quadratic optimization problem:

$$\text{minimize:} \frac{\|\mathbf{w}\|^2}{2}$$
$$\text{subject to:} y_i(\mathbf{x}_i^T\mathbf{w} + w_0) \geq 1. \tag{4.2}$$

Lagrange function for this problem is:

$$J(\mathbf{w}, w_0, \boldsymbol{\alpha}) = \frac{1}{2}\|\mathbf{w}\|^2 - \sum_{i=1}^{n} \alpha_i \left[y_i(\mathbf{x}_i^T\mathbf{w} + w_0) - 1 \right], \tag{4.3}$$

where $\alpha_i, i = 1, \ldots, n$ are Lagrange multipliers. Thus, the problem can be stated as:

$$\text{minimize:} J(\mathbf{w}, w_0, \boldsymbol{\alpha}) \text{ with respect to } \mathbf{w}, w_0$$
$$\text{subject to:} \alpha_i \geq 0. \tag{4.4}$$

Then, the equivalent dual problem is:

$$\text{maximize:} J(\mathbf{w}, w_0, \boldsymbol{\alpha}) \text{ with respect to } \boldsymbol{\alpha}$$
$$\text{subject to:} \alpha_i \geq 0. \tag{4.5}$$

By imposing the Kuhn-Tucker stationary conditions on the dual problem (4.5) we obtain:

$$\nabla_{\mathbf{w}} J(\mathbf{w}, w_0, \boldsymbol{\alpha}) = \mathbf{w} - \sum_{i=1}^{n} \alpha_i y_i \mathbf{x}_i = 0$$
$$\frac{\partial J(\mathbf{w}, w_0, \boldsymbol{\alpha})}{\partial w_0} = -\sum_{i=1}^{n} \alpha_i y_i = 0 \tag{4.6}$$

Using (4.4)–(4.6) the dual problem can be stated as:

$$\text{maximize:} J(\boldsymbol{\alpha}) = \sum_{i=1}^{n} \alpha_i - \frac{1}{2}\sum_{i,j=1}^{n} \alpha_i \alpha_j y_i y_j (\mathbf{x}_i^T \mathbf{x}_j)$$
$$\text{subject to:} \alpha_i \geq 0 \text{ and } \sum_{i=1}^{n} \alpha_i y_i = 0. \tag{4.7}$$

The Karush-Kuhn-Tucker (KKT) theorem [60] is the key to the solution of the reduced optimization problem (4.7). Let $\hat{\boldsymbol{\alpha}}$ be a solution of the problem. Then $\hat{\mathbf{w}}$ can be determined from (4.6):

$$\hat{\mathbf{w}} = \sum_{i=1}^{n} \hat{\alpha}_i y_i \mathbf{x}_i \tag{4.8}$$

KTT conditions guarantee that $\hat{\alpha}_i > 0$ only for the support vectors, i.e. feature vectors that lie on the canonical hyperplanes H_1 and H_2. Therefore, $\hat{\mathbf{w}}$ is a linear combination of support vectors only. The support vectors are the most important elements in the training set, since they define the separating hyperplane $\hat{\mathbf{w}}^{\mathrm{T}}\mathbf{x} + \hat{w}_0$. The removal of the rest of the training vectors would not affect the outcome of the training.

All of the above holds true under the separability assumption. In a non-separable case, (4.1) constraints are relaxed by introducing non-negative slack variables $\xi_i, i = 1, \ldots, n$, and a cost coefficient C [61]. Thus, the new constraints are

$$\begin{aligned} \mathbf{x}_i^{\mathrm{T}}\mathbf{w} + w_0 &\geq +1 - \xi_i, \text{ for } y_i = +1 \\ \mathbf{x}_i^{\mathrm{T}}\mathbf{w} + w_0 &\leq -1 + \xi_i, \text{ for } y_i = -1, \end{aligned} \tag{4.9}$$

and the optimization problem becomes:

$$\begin{aligned} \text{minimize:} &\quad \frac{\|\mathbf{w}\|^2}{2} + C\sum_{i=1}^{n} \xi_i \\ \text{subject to:} &\quad \xi_i \geq 0 \text{ and } y_i(\mathbf{x}_i^{\mathrm{T}}\mathbf{w} + w_0) \geq 1 - \xi_i. \end{aligned} \tag{4.10}$$

The cost parameter C is set by a user, and it acts as an upper bound for Lagrange multipliers α_i in the dual formulation. Larger C leads to higher penalty for an error. Generalization of the cost coefficient into two coefficients, which depend on the type of the error, provides control over sensitivity of the classifier [62].

Training of Support Vector classifiers is performed numerically. The data in this research was trained using LIBSVM toolbox [63]. LIBSVM implements the decomposition method described in [63, 64].

After training produces the optimal hyperplane, feature vectors are assigned classes depending on which side of the hyperplane they lie. The following decision function is used for classification of both, separable and non-separable cases:

$$D(\mathbf{x}) = \text{sign}\left(\hat{\mathbf{w}}^\text{T}\mathbf{x} + \hat{w}_0\right) = \text{sign}\left(\sum_{\substack{\text{support}\\\text{vectors}}} \hat{\alpha}_i y_i \mathbf{x}_i^\text{T}\mathbf{x} + \hat{w}_0\right) \tag{4.11}$$

4.2.2 Decision Tree Induction

Decision tree classifiers can be characterized by their property of breaking a complex classification task into a collection of simple hierarchical rules. These rules are represented in the form of a tree where the root and each internal node test a condition on the features and each edge is marked with a distinct outcome of that test. The leaf nodes contain either a predicted class label in case of classification trees or a predicted value from the output domain in case of regression trees.

Given the training and testing data, the objective is to design a decision tree based on a training set so that it would best generalize over the testing set, have low misclassification error and simplest structure. The misclassification error can be estimated simply by taking the ratio of misclassified test samples to the total number of test samples. However, in this research the following misclassification cost function was used to estimate the misclassification error given the data set:

$$R(T) = \sum_{t \in \text{leaves}(T)} p(t)R(t), \tag{4.12}$$

where leaves(T) is the set of leaves of the tree T, $p(t)$ is the estimated probability of the leaf t, $R(t)$ is the ratio of misclassified samples to the total number of observed samples in that node. The design of a tree involves designing the structure of the tree and choosing criteria for each node split, i.e. selecting the features and the decision rule which will be used in the evaluation of the node outcome.

Top-Down Induction of Decision Trees (TDIDT) [65, 66] is one of the most effective approaches in learning the structure of decision trees. The tree is constructed by selecting node splitting rules starting with the root and proceeding down to the leaves until further

splitting does not improve classification accuracy. This results in a large tree which is then optimized by pruning the subtrees that have little impact on generalization accuracy. The design of decision trees used in this research is restricted to binary structures, since it was shown that any ordered tree can be transformed into equivalent binary tree [67].

The node splits pursue the goal of making the data in the child nodes purer, i.e. composed of fewer classes. The Gini index of diversity $G(t)$ was used as an impurity function for node splitting in [66]:

$$G(t) = \sum_{I \neq J} p(I|t)p(J|t), \tag{4.13}$$

where $p(I|t)$ is the probability of a sample $\mathbf{x}$ belonging to class I given we are at the node t. We are dealing with a binary classification problem, thus, the Genie index takes the following form:

$$G(t) = p(T|t)p(\neg T|t) \tag{4.14}$$

The split that produces the largest decrease in purity is selected among all candidate splits. The decrease in impurity caused by the split S in node t is defined as:

$$\Delta G(S,t) = G(t) - G(t_L)p_L - G(t_R)p_R, \tag{4.15}$$

where t_L is the left child of t, t_R is the right child, p_L is the proportion of cases that go into the left child.

It was suggested in [66] that the stopping rules are more important in tree design than the splitting rules. We have taken the threshold for the maximal decrease in purity as a criterion for stopping the splits:

$$\max_{S,t} \Delta G(S,t) < \theta. \tag{4.16}$$

However, substantially small threshold have been used, so that the leafs are completely or almost completely pure, and the final tree is large enough for effective pruning.

Let T_t be a subtree of a tree T, that consists of $t \in T$ and its all descendants in T. Define the pruned tree $T - T_t$ as the tree which is obtained from T by removing or pruning T_t from

it. If $T\prime$ is obtained from T by successive pruning, denote that partial ordering relation by $T\prime < T$. Define a complexity-cost measure of T as:

$$R_\alpha(T) = R(T) + \alpha \left|\text{leaves}(T)\right|, \tag{4.17}$$

where $R(t)$ is the misclassification error cost of tree T estimated with the given training set and $\alpha > 0$ is the complexity cost. Denote the fully grown tree by $T_{\max}$, and according to [66, 68] for each value of α find the subtree $T(\alpha) \leq T_{\max}$ such that:

$$R_\alpha(T(\alpha)) = \min_{T \leq T_{\max}} R_\alpha(T). \tag{4.18}$$

By forming an increasing sequence of complexity costs $\{\alpha_0, \alpha_1, \ldots, \alpha_L\}$, we obtain a corresponding sequence of pruned $T(\alpha)$ trees $T_0, T_1, \ldots, T_L$. The first element of the former sequence $\alpha_0 = 0$, while α_L is taken large enough, so that the last tree T_L consists of only the root node.

K-fold cross-validation of the training set is used to estimate the misclassification error of the trees in the obtained sequence. In the process of cross-validation the training set is partitioned into K equal or nearly equal subsets with roughly same class proportions. Then nine of those subsets are used to train the tree and the remaining subset is used for testing. The process repeated for each subset and the misclassification error is averaged over 10.

The design and training of decision trees in this work was performed using tree growing and fitting functions in Statistics Toolbox of MATLAB package, which are based on CART algorithm suggested in [66]. The classification of data in a decision trees is done by following the rules from the root to the leaves which contain the class labels.

4.3   WELLNESS MONITORING

The following heuristics is suggested for monitoring of wellness (Fig 15). Define an *adaptive model* $\mathcal{M}_{\mathrm{ad}}$ as a model which is trained using the recognized data for the last k days. $\mathcal{M}_{\mathrm{ad}}$ is used to recognize the target data in the new daily data. A *daily model* $\mathcal{M}_{\mathrm{day}}$ is constructed using a portion of the recognized daily data. $\mathcal{M}_{\mathrm{day}}$ is used to test the recognized data for the last K days and the recognized data for the current day which was not used in the construction of $\mathcal{M}_{\mathrm{day}}$. The difference between the recognition accuracy of the daily target data and the mean recognition accuracy of the previous data by the current daily model is used as the wellness score. The standard deviation of the recognition accuracy of the previous data by the current daily model is used as a confidence score. The subject's condition can be regarded substantially different if the wellness score is more than a standard deviation away from the mean of the wellness scores for the last K days provided that the confidence score is below the acceptable threshold.
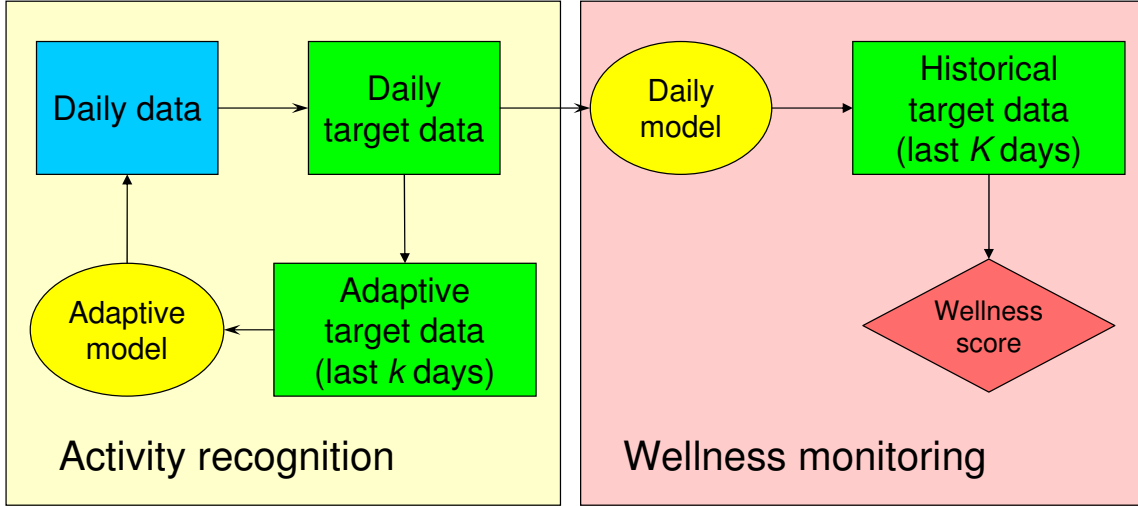
Figure 15: Wellness monitoring algorithm

Suggested algorithm can potentially be used for any data monitoring problem, in which the monitored data should be extracted from a larger data set using some binary classification model. It is universal in the sense that it does not depend on the binary model that is used for recognition of the target data. Specifically, this algorithm can be used for wellness monitoring in the Nursebot, where target data is the data for the target subject and the binary model could be either the gait recognition model, the voice recognition model, or

their combination.

The implementation of the wellness monitoring algorithm using the SenseWear®PRO data is as follows.

- A day is defined as one session. Thus, **the daily data** is the current session data.
- **The adaptive model** is used for activity recognition. It is constructed using the target activity data for the last three days (sessions), i.e. $k = 3$ in Figure 15.
- **The daily model** is constructed from the daily target data that was recognized by the adaptive model.
- The current **wellness score** is obtained as a difference between the recognition accuracy of the current daily target data and the mean recognition accuracy of the target activity data for the last $K = 45$ days by the current daily model. Let $\mathcal{M}(x)$ be the recognition accuracy of data x using a model $\mathcal{M}$, $\tau_j, j = 1, \ldots, K$ be the daily target data j days ago, and τ_0 be the current daily target data. Then

$$\text{wellness score} = \mathcal{M}_{\text{day}}(\tau_0) - \frac{1}{K} \sum_{j=1}^{K} \mathcal{M}_{\text{day}}(\tau_j) \tag{4.19}$$

The sleeping activity is selected as the target activity for recognition and monitoring. However, it could have been any other activity that is frequent and consistent, for example walking with a normal pace. Of the three models used for activity recognition, SVM classifier has been selected as the binary recognition model for testing of the data monitoring algorithm. The results of activity recognition and data monitoring are presented in the next section.

4.4   RESULTS

This section covers the results of application of the activity recognition and wellness monitoring methods to the data collected with SenseWear®PRO armband. The experimental data was collected and made available to the public by BodyMedia. It was obtained in the form

of nine sensory information channels which were described in Section 4.1 and additional contextual information, such as the activity annotation, session number, subject ID, and other user specific physiological characteristics. Only sensory channels and activity annotations were used in activity recognition tasks. The session numbers were taken into account in the wellness monitoring experiments.

Each sample of the sensory channels represents one minute of aggregate data. The activity recognition and monitoring analysis in this section is performed on 30154 samples of annotated data from a single subject, which corresponds to more than 502 hours of data.

4.4.1 Activity Recognition

There are 25 different annotations for activity context marked by the target subject. Each of them is designated a four digit code. For example, 5102 corresponds to a sleeping activity, while 3004 is TV-watching. Figure 16 shows the number of samples labeled with each of the annotations. In this thesis, five different activity recognition tasks are considered, in each of which we concentrate on one of the five most frequent activities: 1103, 2002, 3004, 5102 and 9006.
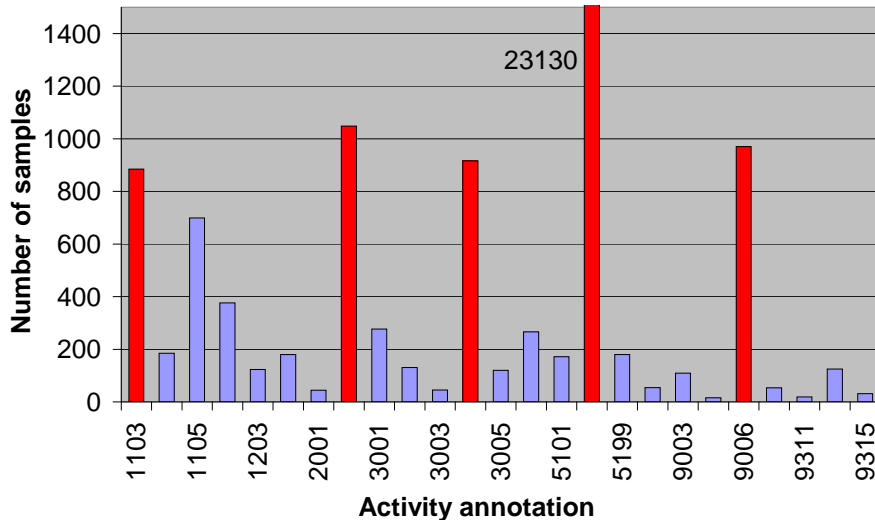
Figure 16: Annotation frequencies. Five most frequent ones (shown in red) are selected as target activities of recognition purposes.

We define a binary recognition problem by assigning positive labels to the target activity

samples and negative labels to the rest of the annotated samples with the exception of ambiguous annotations. Some activity annotations of data are known to be ambiguous, e.g. the annotation 5102 denotes "sleep," but the annotation 5103 may or may not denote "sleep". Given the target activity context we exclude all ambiguous samples from training and testing sets.

For each classification task an equal number of target and non-target activities are selected in order to avoid the bias in classification. Those selected sets are randomly split into training and testing sets with a 70/30 ratio. In addition to that, for each target activity we fix 30 splits for comparison of classification accuracy and sensitivity of the following three methods: SVM, Decision Trees, and Naive Bayes model. However, the training set is too large (4907 samples) for Support Vector Machines in case of the activity 5102. Thus, only a tenth of the training samples is used in that case. The testing set is not altered, therefore, the comparison of classification methods remains valid.

It was noticed that the prediction accuracy of a model based on support vector machines and classification trees was higher, when all of the channels were used, than the predication accuracy of any single channel. Therefore, a stepwise backward elimination method was used for feature selection [69]. Starting with the full set of features, each of the channels is removed from the set, and the accuracy of the classifier is computed based on the above mentioned 30 training/testing splits. The most accurate feature set is selected for the next stage, and the process is repeated. The results of feature selection using stepwise backward elimination for each classification task are shown in Tables 5-14 in Appendix A.

The prediction accuracy of Naive Bayes model with all channels included was worse than the predication accuracy of some channels taken independently. Thus, in case of Naive Bayes model a stepwise forward selection method was applied in order to obtain a better set of features [69]. Starting with an empty feature set, each of the channels is added to the set, and the accuracy of the classifier is computed based on the fixed 30 splits. The most accurate feature set is selected for the next stage, and the process is repeated. The results of feature selection using stepwise forward selection for each classification task are shown in Tables 15-19 in Appendix A.

When feature sets are selected for each method and classification task we produce the

confusion matrices and receiver operating characteristic (ROC) curves to assess the sensitivity and specificity of classifiers. A brief explanation of confusion matrices and ROC curves is given in Section 3.3. The confusion matrices for all tasks and methods are given in Tables 20-34 in Appendix B.
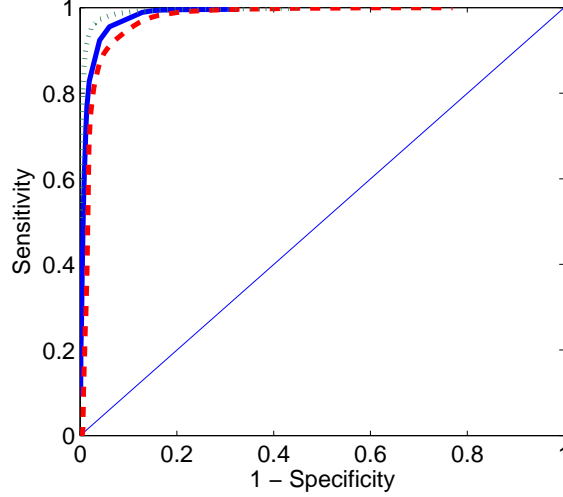
Figure 17: ROC curves of recognition of the activity 5102 using Decision Trees (dotted), Support Vector Machines (solid), and Naive Bayes classifier (dashed).

The ROC curves for Naive Bayes model were produced by introducing a variable threshold for the difference of the discriminant functions. The sensitivity and specificity of the SVM were adjusted according to [62]. The ROC curve for Decision Trees was obtained by varying the prior probabilities for each class. See Figures 17-20 for comparison of ROC curves for each method and classification task. No ROC curves were produced for the classifiers of the activity 1103, since the classification accuracy and, thus, the sensitivity and specificity of all classifiers were above 99% for that activity.

We would like to keep the false positive rate low, so that a reliable signal for monitoring of the target activity could be obtained. At the same time, a significant drop in true positive rate is also undesirable. It can be seen from the confusion matrices and the ROC curves for all of the activities that the Decision Trees is the most sensitive classifier at low false positives rates. Support Vector Machines exhibit a comparable performance, while Naive Bayes model is the least sensitive of the three classifiers at low false positive rates.

43
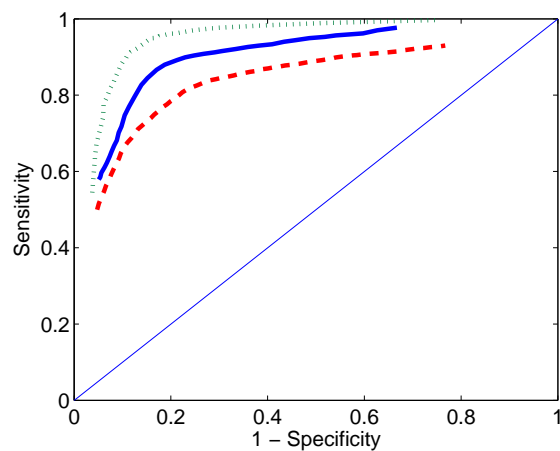
Figure 18: ROC curves of recognition of the activity 3004 using Decision Trees (dotted), Support Vector Machines (solid), and Naive Bayes classifier (dashed).
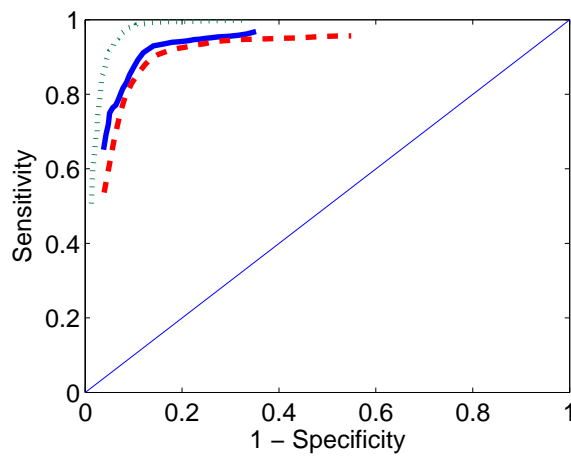
Figure 19: ROC curves of recognition of the activity 2002 using Decision Trees (dotted), Support Vector Machines (solid), and Naive Bayes classifier (dashed).
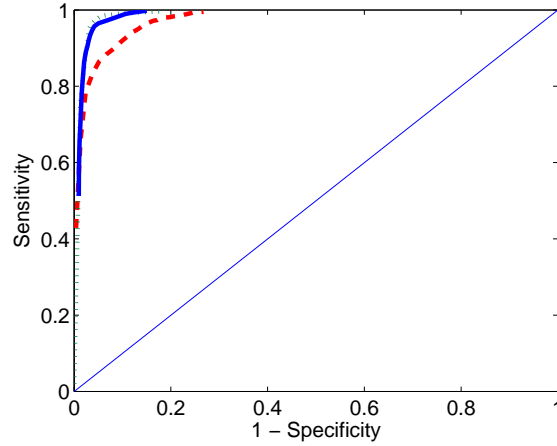
Figure 20: ROC curves of recognition of the activity 9006 using Decision Trees (dotted), Support Vector Machines (solid), and Naive Bayes classifier (dashed).

4.4.2 Wellness Algorithm

The monitoring algorithm described in the Section 4.3 can be used with any binary classifier of activities. SVM is chosen for testing of the algorithm, since it usually performs better with smaller training sets, and Table 25 shows that it is substantially sensitive and accurate at classification of the sleeping activity (5102). The sleeping activity (5102) is selected as the target activity for monitoring, since it is the most frequent activity in the dataset and a regular activity guaranteed to occur every day. In addition, the classifiers can recognize it accurately and sensitively; it is fairly consistent activity, thus, long term wellness problems that affect the monitored biometric traits are likely to be detected during sleep. The feature set shown in Table 8, which is selected according to the backward elimination method outlined above, is used in all data monitoring simulations.

The data was grouped on session basis, i.e. each session is considered to be a "new day". Randomly selected training set of target activity data is used to classify the target data from the first three sessions. The initial *adaptive model* is constructed from the recognized target data. The rest of the process follows the heuristics shown in Figure 15, however, if less than 330 samples are recognized as target activity then the session is ignored, since there is a risk that the amount of data would be insufficient for training of the *daily model* . Only 70% of

45
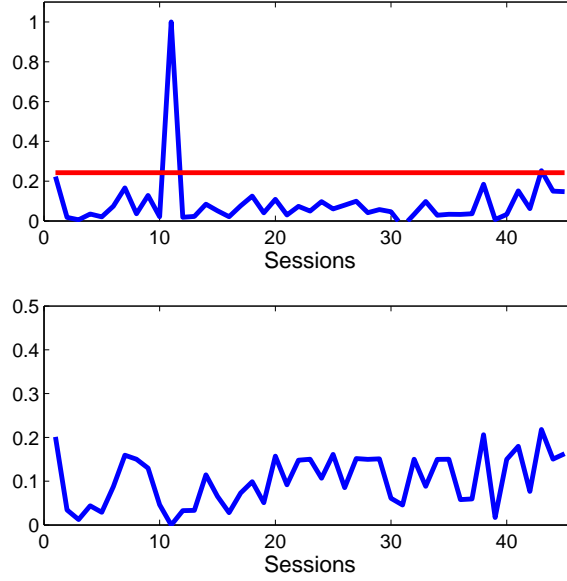
Figure 21: Scores (above) and confidences (below) of the sessions based on the recognized target activity samples.

recognized data is used for training of the daily model, and the remaining 30% is used as a testing set to verify its accuracy. The accuracy and sensitivity of extracting the target data using the adaptive model and the accuracy of the daily model in recognition of the daily testing set were comparable to that of the corresponding activity recognition task shown in Table 25 in Appendix B.

Table 4: Comparison of the averages of session means per feature with the corresponding means of sessions 5, 11, and 43

	1	2	3	4	5	7	8	9
Average	0.4903	6.9283	31.9696	0.0129	31.1633	-0.1686	1.6138	0.0359
Session 5	0.3670	8.2561	31.1710	0.0395	30.1650	-0.2182	2.0507	0.2359
Session 11	**8.0097**	4.8792	32.4850	0.0175	31.4230	-0.0269	1.4485	-0.2613
Session 43	0.2807	4.5967	**33.2470**	0.0000	32.5840	-0.1428	1.8858	0.2092

The scores and their corresponding confidences were obtained according to the wellness monitoring heuristics (Figure 21). The red line on the scores plot marks one standard

46

deviation from the mean of the scores. It can be seen that there are two sessions, 11 and 43, which have scores below the threshold line.
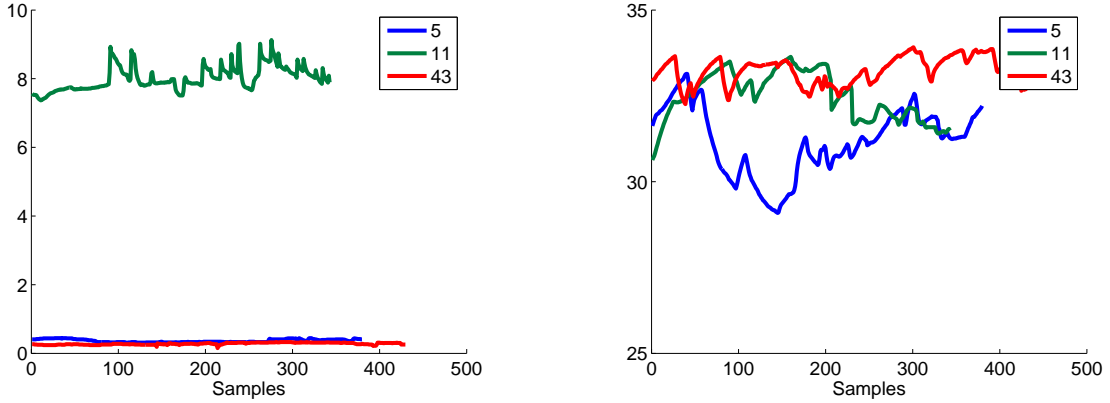
Figure 22: Comparison of features 1 (left) and 3 (right) for session 5, 11, and 43

Quick comparison of the averages of session means per feature with the corresponding means of sessions 5 ("normal" session), 11 and 43 (Table 4) draws the attention to the features 1 and 3 (galvanic skin response and near body temperature). The plots of those channels in Figure 22 demonstrate their deviation from normal in sessions 11 and 43 respectively. In the case of session 11, such a drastic increase of galvanic skin response could have been caused either by sensor malfunction or by intensive sweating. In the case of session 43, higher near-body temperature and, if we take another look at Table 4, somewhat higher skin temperature could be caused by mild fever. Thus, we have shown that the monitoring algorithm is robust enough to reliably recognize the target data and sensitive enough to react to both, large and small anomalies in the feature channels.

5.0   ASSESSMENT OF BALANCE IMPAIRMENT

Parkinson's disease (PD) is a complex neurological disorder that is manifested by a number of symptoms some of which are tremor, rigidity, postural imbalance and bradykinesia [5, 6]. While there are a number of ways to diagnose severe cases of PD, and in many cases it is apparent even to a casual observer, the early diagnosis of PD in risk group patients involve complex medical tests [9, 10].
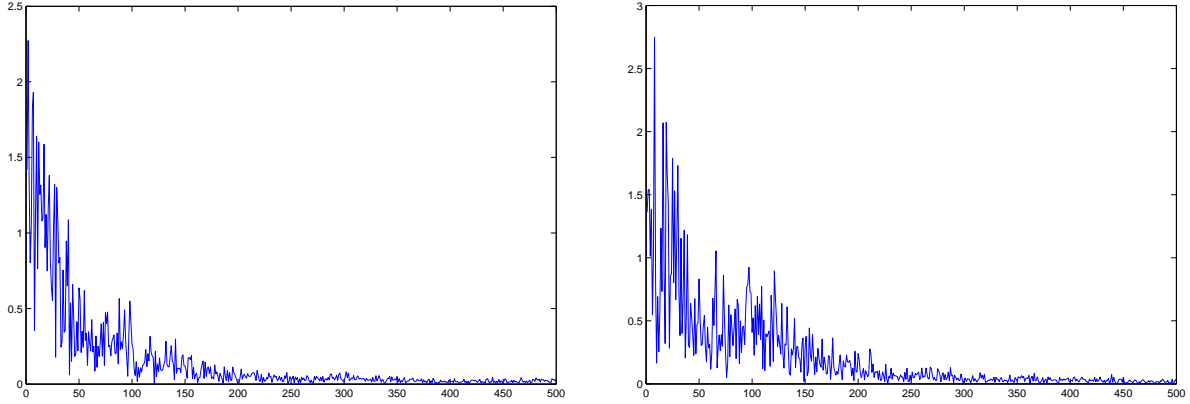
Figure 23: Spectrum of a signal from a normal subject (left) and from a Parkinsonian subject (right)

The goal of this research is to develop a measure of balance impairment that would identify early stages of non-clinical PD. This is done by classification of the data collected from PD patients, first degree relatives of PD patients, and normal control subjects using electronic force platform.

The electronic platform records the position of the center of pressure beneath the feet of a subject at sampling rate of 50 Hz. The data previously has been analyzed using auto-covariance and related autocorrelation function [70]. In here we discuss a spectral analysis

approach.

We assume that the x and y coordinates of the center of pressure in our time series are independent. Therefore, we process the data one coordinate at a time. First we take Discrete Fourier Transform of each signal:

$$X(k) = \sum_{n=0}^{N-1} x(n)e^{-i\frac{2\pi}{N}nk}. \tag{5.1}$$

The spectral data then is binned into ten equally spaced bins.

$$B_k = \sum_{n=1+(k-1)N/10}^{kN/10} X(n), \text{ where } k = 1, \ldots, 10. \tag{5.2}$$

Then we form partial sums P_i of bins:

$$P_i = \sum_{k=1}^{i} B_k, \text{ where } i = 1, \ldots, 10. \tag{5.3}$$
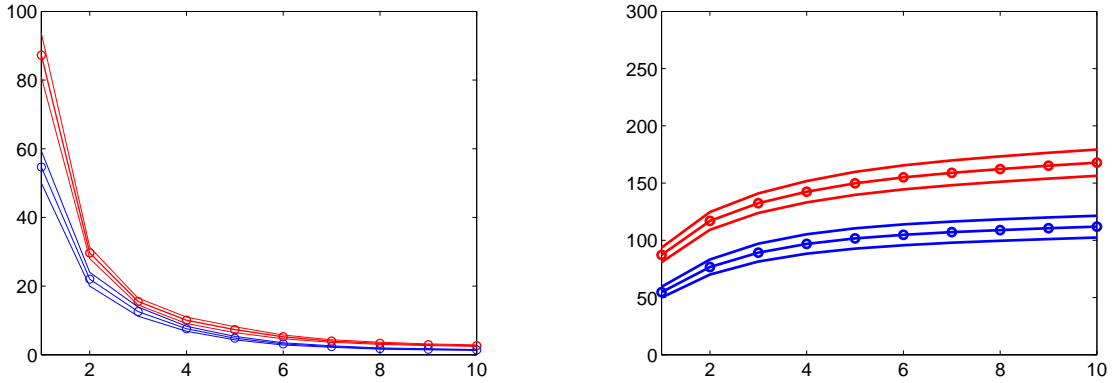
Figure 24: Means of binned data (left) and means of partial sums (right) with confidence bands formed with standard deviations. Red is for Parkinsonian subjects, and the blue is for the normal subjects.

We have processed data collected from 17 parkinsonian subjects and 10 normal subjects using the above methods. The data on each subject was recorded in five two minute long sessions. As it can be seen from the means of binned data and partial sums across the total class of normal/parkinsonian subjects on Figure 24 the center of pressure obtained for electronic platforms exhibits substantial discriminating power.

We have also determined that spectral data combined with other measures of the platform data such as autocovariance can identify some first degree relatives of PD patients. The next logical step in this research would be the comparison of balance impairment measure obtained from electronic platform data with positron emission tomography scans mappings of amounts of dopamine in the brain. This way we can determine whether force platform measures can be reliably used for preventive diagnostics of preclinical PD.

6.0 CONCLUSIONS AND FUTURE WORK

Three applications of machine learning to the problems in biometric data analysis have been examined in this thesis. Significant contributions have been made in the areas of automatic gait recognition, model-based data monitoring, and early medical diagnostics. These contributions have been validated with corpora of data collected in laboratory conditions and in the real world environment.

A multimodal system for biometric analysis that relies on data from two audio and one vibration channel has been constructed. It has been shown that the non-subject data can be filtered out using a multimodal biometric system based on voice and gait. The gait analysis subsystem indicated that information fusion of audio and vibration channels improved the performance of the system.

A novel approach in gait recognition, based on audio and vibration of the foot impact with the floor, has been introduced. The advantage of that method over traditional video-based automatic gait recognition is that it is independent of the viewing angle, background, and the clothing of the person. Experimental results of our approach using the data collected in laboratory conditions have been very promising. These results (Table 1) suggest that our method can be sufficiently accurate for person verification and wellness analysis tasks.

A speaker recognition system based on the Gaussian Mixture Model has been implemented. The system has been tested in low-noise laboratory conditions, and it has proved to be very accurate in recognition tasks with a small number of subjects. We expect the nursebot to be placed in nursing institutions and residences of elderly people where noise conditions are comparable to those in our experiments and the universe of visitors is limited to friends, family, and health care personnel.

The primary goal of this research has been automatic monitoring of wellness. I have

51

developed and implemented a novel algorithm for data monitoring based on a binary recognition model. The proposed heuristics is unique since it can be applied in any monitoring system in which a pattern recognition model is successful at separating the monitored data from a larger data set. The algorithm was tested on a large corpus of real world data collected by Bodymedia, Inc. using SenseWear®PRO armband device.

It has been shown that the recognition of the activity context of a person wearing a SenseWear®PRO armband can be reliably performed with the Decision Trees, Support Vector Machines, and Naive Bayes Model (Tables 20-34). Support Vector Machines has been used as the binary recognition model in data monitoring experiments. The anomalous data sets in the target data have been successfully identified using the monitoring algorithm.

The possibilities of future research in the area of biometric data recognition and monitoring are abundant. In view of my results in gait recognition using audio and vibration, the gait can be turned into an important biometric in authentication and diagnostic applications. Another natural direction for future research would be to collect a larger data set using the data acquisition system designed for the nursebot and test it with the wellness monitoring algorithm.

Automatic monitoring of a person's wellness with a wearable device introduces a new paradigm in wearable computing, in which a person does not necessarily control the device, but the device rather augments the autonomic nervous system. Thus, data monitoring using wearable technology is another interesting area for future research.

Finally, the results obtained in this thesis encourage research in biomedical data analysis. Detection of the clinically relevant information in that data is the biggest challenge in the field. Thus, further investigation of biomedical data using the contemporary computational power can have a significant impact on the cost and quality of health care.

APPENDIX A

FEATURE SELECTION TABLES

Table 5: Feature selection for recognition of the activity 3004 with Decision Trees

			Channels						Accuracy
1	2	3	4	5	6	7	8	9	0.8920
1	2	3	4	5	6	7	9		0.8942
1	**2**	**3**	**4**	**5**	**7**	**9**			**0.8957**
1	2	3	5	7	9				0.8954
2	3	5	7	9					0.8901
2	5	7	9						0.8854
2	7	9							0.8719
2	7								0.8485

Table 6: Feature selection for recognition of the activity 3004 with Support Vector Machines

1	2	3	4	Channels 5	6	7	8	9	Accuracy
1	**2**	**3**	**4**	**5**	**6**	**7**	**8**	**9**	**0.8437**
1	2	3	4		6	7	8	9	0.8418
	2	3	4		6	7	8	9	0.8416
	2	3	4		6	7	8		0.8408
	2	3			6	7	8		0.8405
	2	3			6	7			0.8388
	2				6	7			0.8255
					6	7			0.8204

Table 7: Feature selection for recognition of the activity 5102 with Decision Trees

1	2	3	4	Channels 5	6	7	8	9	Accuracy
1	2	3	4	5	6	7	8	9	0.9663
1	**2**	**3**	**4**	**5**	**6**	**7**		**9**	**0.9675**
1	2	3		5	6	7		9	0.9669
1	2			5	6	7		9	0.9661
1	2				6	7		9	0.9645
1	2					7		9	0.9598
	2					7		9	0.9542
	2					7			0.9428

Table 8: Feature selection for recognition of the activity 5102 with Support Vector Machines

				Channels					Accuracy
1	2	3	4	5	6	7	8	9	0.9469
1	**2**	**3**	**4**	**5**	**7**	**8**	**9**		**0.9470**
1	2	3	5	7	8	9			0.9466
2	3	5	7	8	9				0.9461
2	3	5	7	8					0.9461
2	3	7	8						0.9431
2	7	8							0.9423
2	7								0.9364

Table 9: Feature selection for recognition of the activity 2002 with Decision Trees

				Channels					Accuracy
1	2	3	4	5	6	7	8	9	0.9451
1	2	3	4	5	6	7	9		0.9460
1	**2**	**3**	**4**	**6**	**7**	**9**			**0.9472**
1	2	4	6	7	9				0.9454
1	4	6	7	9					0.9450
1	6	7	9						0.9424
6	7	9							0.9360
6	7								0.9220

Table 10: Feature selection for recognition of the activity 2002 with Support Vector Machines

Channels									Accuracy
1	2	3	4	5	6	7	8	9	0.8940
1	2	3	4	5	6	7	9		0.8963
2	**3**	**4**	**5**	**6**	**7**	**9**			**0.8987**
2	3	4	5	6	7				0.8971
3	4	5	6	7					0.8956
4	5	6	7						0.8956
4	5	7							0.8964
4	7								0.8948

Table 11: Feature selection for recognition of the activity 1103 with Decision Trees

Channels									Accuracy
1	2	3	4	5	6	7	8	9	0.9991
2	3	4	5	6	7	8	9		0.9991
3	4	5	6	7	8	9			0.9991
4	5	6	7	8	9				0.9991
5	6	7	8	9					0.9991
6	7	8	9						0.9991
6	8	9							0.9991
6	**9**								**0.9991**

Table 12: Feature selection for recognition of the activity 1103 with Support Vector Machines

Channels									Accuracy
1	2	3	4	5	6	7	8	9	0.9979
1	3	4	5	6	7	8	9		0.9986
1	4	5	6	7	8	9			0.9988
4	5	6	7	8	9				0.9989
4	6	7	8	9					0.9988
4	6	7	9						0.9991
6	**7**	**9**							**0.9992**
6	7								0.9991

Table 13: Feature selection for recognition of the activity 9006 with Decision Trees

Channels									Accuracy
1	2	3	4	5	6	7	8	9	0.8826
1	2	3	5	6	7	8	9		0.9646
1	**2**	**3**	**5**	**6**	**7**	**9**			**0.9659**
1	3	5	6	7	9				0.9653
1	3	6	7	9					0.9655
1	3	6	7						0.9602
3	6	7							0.9534
6	7								0.9411

Table 14: Feature selection for recognition of the activity 9006 with Support Vector Machines

Channels									Accuracy
1	**2**	**3**	**4**	**5**	**6**	**7**	**8**	**9**	**0.9526**
1	3	4	5	6	7	8	9		0.9522
1	3	5	6	7	8	9			0.9518
3	5	6	7	8	9				0.9478
3	5	6	7	9					0.9430
3	5	6	7						0.9309
5	6	7							0.9112
6	7								0.9104

Table 15: Feature selection for recognition of the activity 3004 with Naive Bayes Model

Channels									Accuracy
1	2	3	4	5	6	7	8	9	0.6144
7									0.7799
7	6								0.8267
7	6	4							0.8268
7	6	4	8						0.8218
7	6	4	8	2					0.7813
7	6	4	8	2	9				0.7499
7	6	4	8	2	9	1			0.6873

Table 16: Feature selection for recognition of the activity 5102 with Naive Bayes Model

				Channels					Accuracy
1	2	3	4	5	6	7	8	9	0.9228
7									0.9165
7	**2**								**0.9278**
7	2	4							0.9275
7	2	4	1						0.9265
7	2	4	1	9					0.9253
7	2	4	1	9	6				0.9255
7	2	4	1	9	6	5			0.9250

Table 17: Feature selection for recognition of the activity 2002 with Naive Bayes Model

				Channels					Accuracy
1	2	3	4	5	6	7	8	9	0.7011
7									0.8593
7	**4**								**0.8741**
7	4	6							0.8666
7	4	6	1						0.8584
7	4	6	1	8					0.8353
7	4	6	1	8	3				0.7946
7	4	6	1	8	3	5			0.7467

Table 18: Feature selection for recognition of the activity 1103 with Naive Bayes Model

			Channels						Accuracy
1	2	3	4	5	6	7	8	9	0.9980
6									0.9981
6	**1**								**0.9982**
6	1	9							0.9982
6	1	9	3						0.9982
6	1	9	3	5					0.9982
6	1	9	3	5	7				0.9981
6	1	9	3	5	7	8			0.9980

Table 19: Feature selection for recognition of the activity 9006 with Naive Bayes Model

			Channels						Accuracy
1	2	3	4	5	6	7	8	9	0.5362
7									0.8828
7	**9**								**0.9049**
7	9	8							0.8991
7	9	8	6						0.8884
7	9	8	6	4					0.8814
7	9	8	6	4	2				0.8608
7	9	8	6	4	2	1			0.7987

APPENDIX B

CONFUSION MATRICES

Table 20: Confusion matrix of recognition of the activity 3004 with Naive Bayes Model

		Actual	
		Target	Other
Prediction	Accept	39.03%	6.35%
	Reject	10.97%	43.65%

Table 21: Confusion matrix of recognition of the activity 3004 with Decision Trees

		Actual	
		Target	Other
Prediction	Accept	45.16%	5.59%
	Reject	4.84%	44.41%

Table 22: Confusion matrix of recognition of the activity 3004 with Support Vector Machines

		Actual	
		Target	Other
Prediction	Accept	42.29%	7.92%
	Reject	7.71%	42.08%

Table 23: Confusion matrix of recognition of the activity 5102 with Naive Bayes Model

		Actual	
		Target	Other
Prediction	Accept	45.55%	2.77%
	Reject	4.45%	47.23%

Table 24: Confusion matrix of recognition of the activity 5102 with Decision Trees

		Actual	
		Target	Other
Prediction	Accept	48.43%	1.68%
	Reject	1.57%	48.32%

Table 25: Confusion matrix of recognition of the activity 5102 with Support Vector Machines

		Actual	
		Target	Other
Prediction	Accept	47.64%	2.94%
	Reject	2.36%	47.06%

Table 26: Confusion matrix of recognition of the activity 2002 with Naive Bayes Model

		Actual	
		Target	Other
Prediction	Accept	42.84%	5.43%
	Reject	7.16%	44.57%

Table 27: Confusion matrix of recognition of the activity 2002 with Decision Trees

		Actual	
		Target	Other
Prediction	Accept	48.21%	3.49%
	Reject	1.79%	46.51%

Table 28: Confusion matrix of recognition of the activity 2002 with Support Vector Machines

		Actual	
		Target	Other
Prediction	Accept	46.21%	6.9%
	Reject	3.79%	43.1%

Table 29: Confusion matrix of recognition of the activity 1103 with Naive Bayes Model

		Actual	
		Target	Other
Prediction	Accept	49.93%	0.11%
	Reject	0.07%	49.89%

Table 30: Confusion matrix of recognition of the activity 1103 with Decision Trees

		Actual	
		Target	Other
Prediction	Accept	49.93%	0.02%
	Reject	0.07%	49.98%

Table 31: Confusion matrix of recognition of the activity 1103 with Support Vector Machines

		Actual	
		Target	Other
Prediction	Accept	49.93%	0.01%
	Reject	0.07%	49.99%

Table 32: Confusion matrix of recognition of the activity 9006 with Naive Bayes Model

		Actual	
		Target	Other
Prediction	Accept	43.03%	2.54%
	Reject	6.97%	47.46%

Table 33: Confusion matrix of recognition of the activity 9006 with Decision Trees

		Actual	
		Target	Other
Prediction	Accept	48.8%	2.21%
	Reject	1.2%	47.79%

Table 34: Confusion matrix of recognition of the activity 9006 with Support Vector Machines

		Actual	
		Target	Other
Prediction	Accept	48.6%	3.34%
	Reject	1.4%	46.66%

BIBLIOGRAPHY

[1] US Census Bureau, "U.S. interim projections by age, sex, race, and hispanic origin." http://www.census.gov/ipc/www/usinterimproj/natprojtab01b.pdf, 2000.

[2] R. O. Duda, P. E. Hart, and D. G. Stork, *Pattern Classification*. Wiley, 2 ed., 2001.

[3] J. D. M. Ashbourn, *Biometrics: Advanced Identify Verification: The Complete Guide*. Springer, 2000.

[4] BodyMedia, "SenseWear®PRO$_2$ Armband." http://www.bodymedia.com/research/sensewear.jsp, 2004.

[5] D. J. Gelb, E. Oliver, and S. Gilman, "Diagnostic criteria for Parkinson's disease," *Arch Neurol*, vol. 56, pp. 33–39, 1999.

[6] J. Sian, M. Gerlach, M. Youdim, and P. Riederer, "Parkinson's disease: a major hypokinetic basal ganglia disorder," *Journal of Neural Transmission*, vol. 106, p. 44376, 1999.

[7] A. Schapira, "Nuclear and mitochondrial genetics in Parkinson's disease," *Journal of Medical Genetics*, vol. 32, pp. 411–414, 1995.

[8] S. Fahn and R. Elton, *Developments in Parkinson's Disease*, vol. II, ch. The unified Parkinson's disease rating scale, pp. 153–169. Florham Park, NJ: Macmillan Healthcare Information, 1987.

[9] S. Starkstein and R. Leiguarda, "Neuropsychological correlates of brain atrophy in Parkinson's disease: a ct-scan study," *Movement Disorders*, vol. 8, no. 1, pp. 51–5, 1993.

[10] T. Brucke, S. Djamshidian, G. Bencsits, W. Pirker, S. Asenbaum, and I. Podreka, "Spect and pet imaging of the dopaminergic system in Parkinson's disease," *Journal of Neurology*, vol. 247, no. IV, pp. 2–7, 2000.

[11] A. Lees, "Drugs for Parkinson's disease," *Journal of Neurology Neurosurgery and Psychiatry*, vol. 73, pp. 607–610, 2002.

[12] A. K. Jain, A. Ross, and S. Prabhakar, "An introduction to biometric recognition," *IEEE Transactions on Circuits and Systems for Video Technology*, vol. 14, pp. 4–20, 2004.

[13] L. Hong, A. K. Jain, and S. Pankanti, "Can multibiometrics improve performance?," *Proceedings of AutoID'99: IEEE Workshop on Automated ID Technologies*, pp. 59–64, 1999.

[14] R. Brunelli and D. Falavigna, "Person identification using multiple cues," *IEEE Transactions on Pattern Analysis and Machine Intelligence*, vol. 17, no. 10, pp. 955–966, 1995.

[15] L. Wald, *Data fusion: definitions and architectures - fusion of images of different spatial resolutions.* Les Presses de l'Ecole des Mines, 2002.

[16] G. Shakhnarovich, L. Lee, and T. Darrell, "Integrated face and gait recognition from multiple views," *Proceedings of the 2001 IEEE Computer Society Conference on Computer Vision and Pattern Recognition*, vol. 1, pp. I439–I446, 2001.

[17] J. Perry, *Gait Analysis: Normal and Pathological Function.* Slack, 1992.

[18] O. A. Kuchar, Y. L. Lazukova, D. Riordan, and J. L. Leahey, "A case-based reasoning system involving a quantized method for gait disorder diagnosis," *IASTED International Conference on Artificial Intelligence and Soft Computing*, pp. 367–370, 1998.

[19] P. Tsai, M. Shah, K. Keiter, and T. Kasparis, "Cyclic motion detection for motion based recognition," *Pattern Recognition*, vol. 27, no. 12, pp. 1591–1603, 1994.

[20] M. Köhle, D. Merkl, and J. Kastner, "Clinical gait analysis by neural networks - issues and experiences," *Proceedings of IEEE Symposium on Computer-Based Medical Systems*, pp. 138–143, 1997.

[21] M. P. Murray, "Gait as a total pattern of movement," *American Journal of Physical Medicine*, vol. 46, no. 1, pp. 290–332, 1967.

[22] J. Bigun, G. Chollet, and G. Borgefors, *Audio- and Video-based Biometric Person Authentication.* Springer, 1997.

[23] H. Murase and R. Sakai, "Moving object recognition in eigenspace representation: gait analysis and lip reading," *Pattern Recognition Letters*, vol. 17, pp. 155–162, 1996.

[24] P. S. Huang, C. J. Harris, and M. S. Nixon, "Human gait recognition in canonical space using temporal templates," *IEE Proceedings of Vision, Image and Signal Processing*, vol. 146, no. 2, pp. 93–100, 1999.

[25] J. Little and J. Boyd, "Describing motion for recognition," *Videre*, vol. 1, no. 2, pp. 1–32, 1998.

[26] D. Cunado, M. S. Nixon, and J. N. Carter, "Automatic gait recognition via model-based evidence gathering," *Proceedings of AutoID'99: IEEE Workshop on Automated ID Technologies*, pp. 27–30, 1999.

[27] D. Hogg, "Model-based vision: a program to see a walking person," *Image and Vision Computing*, vol. 1, no. 1, pp. 5–20, 1983.

[28] Q. He and C. Debrunner, "Individual recognition from periodic activity using hidden markov models," *IEEE Workshop on Human Motion*, pp. 47–52, 2000.

[29] K. Rohr, "Towards model-based recognition of human movements in image sequences," *Computer Vision, Graphics, and Image Processing: Image Understanding*, vol. 59, no. 1, pp. 94–115, 1994.

[30] K. Davis, R. Biddulph, and S. Balashek, "Automatic recognition of spoken digits," *Journal of the Acoustical Society of America*, vol. 24, pp. 637–642, 1952.

[31] B. Atal, "Automatic recognition of speakers from their voices," *Proceedings of IEEE*, vol. 64, pp. 460–475, 1976.

[32] R. Auckenthaler, M. Carey, and H. Lloyd-Thomas, "Score normalization for text-independent speaker verification systems," *Digital Signal Processing*, vol. 10, pp. 42–54, 2000.

[33] H. A. and D. M., "Glottal fry and voice disguise: a case study in forensic phonetics," *Journal of Biomedical Engineering*, vol. 15, no. 3, pp. 193–200, 1993.

[34] F. Soong, A. Rosenberg, L. Rabiner, and B. Juang, "A vector quantization approach to speaker recognition," *IEEE International Conference on Acoustics, Speech, and Signal Processing*, pp. 387–390, 1985.

[35] T. Kinnunen and P. Fränti, "Speaker discriminative weighting method for VQ-based speaker identification," *Proceedings of 3rd International Conference on audio- and video-based biometric person authentication*, pp. 150–156, 2001.

[36] D. A. Reynolds and R. C. Rose, "Robust text-independent speaker identification using Gaussian mixture speaker models," *IEEE Transactions on Speech and Audio Processing*, vol. 3, pp. 72–82, 1995.

[37] T. Matsui and S. Furui, "Comparison of text-independent speaker recognition methods using VQ-distortion and discrete/continuous HMMs," *IEEE Transactions on Speech and Audio Processing*, vol. 2, pp. 456–459, 1994.

[38] R. A. Gopinath, "Maximum likelihood modeling with Gaussian distributions for classification," *Proceedings of the International Conference on Acoustics, Speech, and Signal Processing*, vol. 2, pp. 661–664, 1998.

[39] J. Oglesby and J. Mason, "Speaker recognition with a neural classifier," *First IEE International Conference on Artificial Neural Networks*, pp. 306 –309, 1989.

[40] K. Farrell, R. Mammone, and K. Assaleh, "Speaker recognition using neural networks and conventional classifiers," *IEEE Transactions on Speech and Audio Processing*, vol. 2, pp. 194 –205, 1994.

[41] S. Mann, "Wearable computing as means for personal empowerment," http://wearcam.org/icwckeynote.html, 1998.

[42] H. N.J., "New method for heart studies: continuous electrocardiography of active subjects over long periods is now practical," *Science*, vol. 134, pp. 1214–20, 1961.

[43] H. Asada, P. Shaltis, A. Reisner, R. Sokwoo, and R. Hutchinson, "Mobile monitoring with wearable photoplethysmographic biosensors," *IEEE Engineering in Medicine and Biology Magazine*, vol. 22, no. 3, pp. 28–40, 2003.

[44] C. Gopalsamy, S. Park, R. Rajamanickam, and S. Jayaraman, "The wearable motherboard: The first generation of adaptive and responsive textile structures (arts) for medical applications," *Journal of Virtual Reality*, vol. 4, pp. 152–168, 1999.

[45] Philips Research, "Philips invents intelligent biomedical clothing for personal healthcare." http://www.research.philips.com/newscenter/archive/2003/pershealth.html.

[46] VivoMetrics, "Lifeshirt® System." http://www.vivometrics.com/site/system.html.

[47] A. Krause, D. Siewiorek, A. Smailagic, and J. Farringdon, "Unsupervised, dynamic identification of physiological and activity context in wearable computing," *Proceedings of the Seventh IEEE International Symposium on Wearable Computers*, pp. 88–97, 2003.

[48] J. M. Jakicic, M. Marcus, K. I. Gallagher, C. Randall, E. Thomas, F. L. Goss, and R. J. Robertson, "Evaluation of the sensewear®PRO$_2$ armband to assess energy expenditure during exercise," *Medicine and Science In Sports and Exercise*, vol. 36, no. 5, pp. 897–904, 2004.

[49] P. Domingos and M. Pazzani, "Beyond independence: Conditions for the optimality of the simple bayesian classifier," *Machine Learning*, vol. 29, pp. 103–130, 1997.

[50] B. S. Atal, "Effectiveness of linear prediction characteristics of the speech wave for automatic speaker identification and verification," *Journal of the Acoustical Society of America*, vol. 55, no. 6, pp. 1304–1312, 1974.

[51] S. B. Davis and P. Mermelstein, "Comparison of parametric representations for monosyllabic word recognition in continuously spoken sentences," *IEEE Transactions on Acoustics, Speech, and Signal Processing*, vol. ASSP-28, no. 4, pp. 357–366, 1980.

[52] I. Jolliffe, *Principal Component Analysis*. Springer, 2 ed., 2002.

[53] S. Haykin, *Neural networks: A comprehensive foundation.* Prentice Hall, 2 ed., 1999.

[54] S. S. Stevens and J. Volkmann, "The relation of pitch of frequency: A revised scale," *American Journal of Psychology*, vol. 53, pp. 329–353, 1940.

[55] A. P. Dempster, N. M. Laird, and D. B. Rubin, "Maximum likelihood from incomplete data via the EM algorithm," *Journal of Royal Statistical Society*, vol. 39, pp. 1–38, 1977.

[56] A. Smailagic and D. Siewiorek, "Application design for wearable and context-aware computers," *IEEE Pervasive Computing*, vol. 1, pp. 20–29, 2002.

[57] G. Abowd, A. Dey, G. Abowd, R. Orr, and J. Brotherton, "Context-awareness in wearable and ubiquitous computing," *Proceedings of International Symposium on Wearable Computers (ISWC'97)*, 1997.

[58] V. Vapnik, *The Nature of Statistical Learning Theory.* Springer Verlag, 1995.

[59] C. J. C. Burges, "A tutorial on support vector machines for pattern recognition," *Data Mining and Knowledge Discovery*, vol. 2, no. 2, pp. 121–167, 1998.

[60] V. Vapnik, *Practical Methods of Optimization.* Wiley, 2 ed., 1987.

[61] C. Cortes and V. Vapnik, "Support-vector networks," *Machine Learning*, vol. 20, no. 3, pp. 273–297, 1995.

[62] K. Veropoulos, N. Cristianini, and C. Campbell, "Controlling the sensitivity of support vector machines," *Proceedings of the International Joint Conference on Artificial Intelligence, (IJCAI99)*, 1999.

[63] C. Chang and C. Lin, "LIBSVM: a library for support vector machines." http://www.csie.ntu.edu.tw/~cjlin/papers/libsvm.pdf, 2004.

[64] E. Osuna, R. Freund, and F. Girosi, "Training support vector machines:an application to face detection," *Proceedings of IEEE conference on computer vision and pattern recognition*, pp. 130–136, 1997.

[65] J. Quinlan, "Induction of decision trees," *Machine Learning*, vol. 1, pp. 81–106, 1986.

[66] L. Breiman, J. Friedman, R. Olshen, , and C. Stone, *Classification and regression trees.* Belmont, CA: Wadsworth Int., 1984.

[67] E. Rounds, "A combined non-parametric approach to feature selection and binary decision tree design," *Pattern Recognition*, vol. 12, pp. 313–317, 1980.

[68] S. Safavian and D. Landgrebe, "A survey of decision tree classifier methodology," *IEEE Trans. Systems, Man, and Cybernetics*, vol. 21, no. 3, pp. 660–674, 1991.

[69] W. Siedlecki and J. Sklansky, "On automatic feature selection," *International Journal of Pattern Recognition and Artificial Intelligence*, vol. 2, no. 2, pp. 197–220, 1988.

[70] G. M. Constantine, N. I. Bohnen, and C. Chow, "Assessing postural rigidity from quiet stance in patients with Parkinson's disease," *Bulletin of the International Statistical Institute*, vol. LIX, no. 2, pp. 147–150, 2001.